Angewandte Chemie
Eine Zeitschrift der Gesellschaft Deutscher Chemiker

Supporting Information

Comprehensive Analysis of Binding Sites in Tubulin

Tobias Mühlethaler[+], Dario Gioia[+], Andrea E. Prota, May E. Sharpe, Andrea Cavalli, and Michel O. Steinmetz**

anie_202100273_sm_miscellaneous_information.pdf
anie_202100273_sm_miscellaneous_information.xlsx

Author Contributions

T.M. designed the research, performed crystallography work, analyzed the data, analyzed published tubulin-protein and tubulin-ligand complex structures, and wrote the paper. D.G. designed the research, performed computational work, analyzed the data, and wrote the paper. A.E.P. designed the research, performed and supervised the crystallography work and analyzed the data. M.E.S. performed crystallography work. A.C. designed the research, supervised the computational work, analyzed the data, and wrote the paper. M.O.S. designed the research, supervised the crystallography work, analyzed the data, wrote the paper, and coordinated the project.

SUPPLEMENTARY INFORMATION

SUPPLEMENTARY MATERIALS AND METHODS

Molecular dynamics (MD) simulation

System preparation. The starting structure of the αβ-tubulin heterodimer for the simulation was extracted from the high-resolution X-ray crystal structure of a protein complex consisting of two αβ-tubulin dimers, the stathmin-like domain of RB3 and tubulin tyrosine ligase (chains C and D of PDB ID 4I4T). The taxane site ligand as well as the calcium and chloride ions were removed. The model contained GTP and GDP molecules bound to the α- and β-tubulin monomers, respectively, as well as their associated Mg^{2+} ions and their coordinating water molecules. The resulting structure possessed 440 out of 451 residues of α-tubulin (UniProtKB ID P81947) and 431 out of 445 residues of β-tubulin (UniProtKB ID Q6B856). Missing residues belonging to the intrinsically disordered C-terminal tails of α- and β-tubulin were not modeled. Residue protonation states were evaluated at pH 7.0 using the Protein Preparation Wizard tool[1] implemented in the Schrödinger 2015-2 suite, and then assigned by visual inspection. A trial protonation at 6.5 (i.e., the pH value of the crystallization condition used for the crystallographic fragment screen; see below) was also carried out, which showed that there is no difference in protonation states between pH 7.0 and 6.5. The αβ-tubulin heterodimer structure was solvated with the TIP3P-model[2] for water molecules in a truncated octahedron box using 12 Å as minimum distance between the protein and the box edges. The system was neutralized by adding Na^+ ions resulting in a total of 123'776 atoms. The atomistic force field Amber-ff99SB-ILDN[3] was used for all simulations. Parameters for Mg^{2+} ions and the GTP and GDP molecules were developed by Allner et al.[4] and Meagher et al.[5], respectively. The αβ-tubulin heterodimer system was assembled with the LEaP tool implemented in the AmberTools 14 software package[6]. Resulting coordinates and topology files have been converted to GROMACS file formats with ACPYPE[7].

MD simulations. MD simulations were performed with GROMACS 4.6.7[8]. The αβ-tubulin heterodimer system was energy minimized using 5'000 cycles of the steepest descent algorithm. Subsequently, the system was equilibrated in four different stages using the V-rescale thermostat[9] and the Parrinello-Rahman barostat[10] with a relaxation time τ of 2 ps and 0.1 ps, respectively, to keep the system at the desired target temperatures and pressure. The first three stages were run for 100 ps each in the NVT

ensemble with an integration time step of 1 fs at the increasing temperature values of 100, 200, and 300 K. For the two initial stages, backbone heavy atoms were harmonically restrained with a force constant of 1'000 kJ/mol/Å^2. The last stage was run in the NPT ensemble for 1 ns with an integration time step of 1 fs. Bonds involving hydrogen atoms were restrained with the LINCS algorithm[11]. A short-range, non-bonded cut-off of 9 Å was applied, whereas long-range electrostatics were treated with the particle mesh Ewald (PME) method[12]. Periodic boundary conditions (PBC) were applied. After the equilibration stage, a 1.1 µs-long MD simulation was conducted with an integration time step of 2 fs in the NPT ensemble at a target temperature and pressure of 300 K and 1 atm, respectively.

Binding pocket analysis. Pockets were identified and tracked over the 1.1 µs of MD simulation by means of the Pocketron[12] module implemented in the BiKi Life Sciences software suite (www.bikitechnologies.com)[13]. The two tubulin monomers were treated separately and the nucleotides, the ions, and the water molecules were removed prior to starting the calculation. Pocket detection is based on the solvent excluded surface concept[14], and performed by rolling a spherical probe of a specific radius over the van der Waals surface of the biomolecular system[12]. Pockets are then identified by calculating the volumetric difference between the regions enclosed by two different solvent excluded surfaces, generated using two different probe radii. In our analysis, we selected the default values of 1.4 and 3.0 Å for the probe radii, and, additionally, the equivalent of five water molecules as cutoff value for the minimum detectable volume (i.e., 34.5 Å^3). These settings have been chosen in order to filter the output and retrieve only those pockets that can be considered as potential fragment or small-molecule ligand binding sites. Because the contact between the α- and β-tubulin monomers generates a large rim, we noticed that, using our analysis criteria, many different pockets at the interface were detected as one extended entity. For this reason, we analyzed the α- and β-tubulin monomers independently from each other. Furthermore, only pockets that were persistent for at least 30 % during the entire simulation or are not located at the intra-dimer interface of αβ-tubulin were taken into account. One pocket involved the actual, artificial C-terminus of the β-tubulin structure (see above); it was thus not further considered.

Protein preparation, crystallographic fragment screening and structure refinement

Protein purification and T_2R-TTL complex formation was performed as previously described[15]. To produce T_2R-TTL complex crystals, 400 nL drops at a 1:1 protein:reservoir ratio were set up in MRC3 vapor-diffusion

plates (Swissci AG) at 20°C in a precipitant solution consisting of 2% PEG 4K, 4 % glycerol, 30 mM $MgCl_2$, 30 mM $CaCl_2$, 100 mM MES/imidazole, pH 6.5, 5 mM L-tyrosine.

Suitable drops for fragment screening were chosen using the TeXRank software package[16]. An Echo 550 instrument (Labcyte) was used to dispense the DSI-poised fragment library[17] (see also https://www.diamond.ac.uk/Instruments/Mx/Fragment-Screening/New_Fragment-Libraries/DSi-Poised-Library.html). To the best of our knowledge, none of the fragments present in this library are known to bind to tubulin. Fragments were dispensed into the selected crystal drops to a final concentration of 100 mM fragment and 20% DMSO. After 1h soaking time, the crystals were mounted on loops using the Crystal Shifter Device (Oxford Lab Technologies) and subsequently cryo-cooled in liquid nitrogen. Native data sets were collected at 100 K at beamline I04-1 at the Diamond Light Source (Harwell Science and Innovation Campus, Didcot, UK). Data were processed using autoPROC[18].

Structures were determined by the difference Fourier method using the phases of the T_2R-TTL complex (PDB ID 5LXT) in the absence of ligands and solvent molecules as a starting point for refinement. The models were first fitted by several cycles of rigid body refinement followed by simulated annealing and restrained refinement in Phenix[19]. Well defined electron densities at contour levels of both 1.0 σ (2mFo-DFc) and 3.0 σ (mFo-DFc) and 50% occupancy upon refinement were chosen as selection threshold for modeling the bound fragments. Ligands were built with Coot's Lidia and the resulting models were further improved using Coot[20]. MolProbity was used to assess the quality of the structures[21]. Chains in the T_2R-TTL complex were defined as follows: chain A, α1-tubulin; chain B, β1-tubulin; chain C, α2-tubulin; chain D, β2-tubulin; chain E, RB3; chain F, TTL.

Structure visualization, molecular editing and figure preparation were performed with the PyMOL molecular graphics system (The PyMOL Molecular Graphics System, Version 2.2.3 Schrödinger, LLC). Fragment volumes were calculated using the volume_calc.py script of the Schrödinger Suite. Notably, two fragments bound to a site formed at the interface between the RB3 and α2-tubulin and another fragment bound to a site located between α2-tubulin and a symmetry related tubulin molecule in the crystal. These three fragments were not further considered for our analysis and denoted as X1 and X3 in Table S3. In addition, three fragments have a second binding site formed by a symmetry related tubulin or TTL, which was not counted as an additional binding site. No fragments bound to TTL.

Analysis of tubulin-tubulin and tubulin- or microtubule-protein contact points

The Protein Data Bank (PDB) was exhaustively searched for tubulin and microtubule structures with a resolution <4.5 Å for X-ray crystallography structures and <8 Å for cryo-electron microscopy structures. For the tubulin-tubulin contact point analysis in the context of the microtubule lattice, we superimposed the α- or β-tubulin monomers of the T_2R-TTL complex onto the corresponding ones in a microtubule. Residues within 4 Å distance from an adjacent tubulin monomer in the microtubule lattice were then identified using PyMOL and compared to the residues forming a computationally predicted pocket or an experimentally determined fragment site. For the tubulin- and microtubule-protein contact point analysis, we superimposed the α- or β-tubulin monomers of the T_2R-TTL complex onto the tubulin monomers to which a protein partner was bound. Subsequently, the same analysis as for tubulin-tubulin contact points was performed. A contact-point overlap is considered in cases where >20% of the residues forming a pocket or site are at a maximal distance of 4 Å from interacting residues of a binding partner (i.e., α-tubulin, β-tubulin or protein partner). Superimposition of "curved" onto "straight" tubulin structures was performed as previous reported[22] by including only residues of the corresponding N- and C-terminal domains of a tubulin monomer.

SUPPLEMENTARY FIGURE LEGENDS

Figure S1. MD simulation.

Calculated root mean square deviations (RMSD) of the Cα atoms of the αβ-tubulin heterodimer from the initial X-ray structure plotted as a function of time with (red) and without (blue) the H1-S2, M, and S9-S10 loops of both tubulin monomers. The lighter color represents the effective sampling of the RMSD during the simulation, whereas the darker lines have been obtained to approximate the data with a Bezier curve in order to cut off noise.

Figure S2. Electron densities of T_2R-TTL-fragment complex structures.

For each fragment, the location of the fragment within the two αβ-tubulin heterodimers of the T_2R-TTL complex is shown on the left. For simplicity, the RB3 and TTL molecules were omitted. The α- and β-tubulin monomers are shown in ribbon representation and colored in dark and light gray, respectively. Fragments are shown in orange sphere representation. Electron-density maps of the fragments are shown on the right. The SigmaA-weighted 2mFo-DFc (dark blue mesh) and mFo-DFc (light green mesh) omit maps are contoured at +1.0 σ and +3.0 σ, respectively. The map calculations excluded the atoms of the ligand.

Figure S3. Chemical structures of fragments.

The chemical structures of the 59 fragments identified in our crystallographic screen are ordered by sIDs and fragment IDs (see also Table S2 and Table S3). Fragments binding as pairs two times to the same site and/or binding to another sID are labeled accordingly. Identical fragment moieties that were experimentally found to interact in a similar manner with residues forming a site are defined as common "binding motif" and are highlighted in blue (see also Figure 3).

SUPPLEMENTARY REFERENCES

[1] G. M. Sastry, M. Adzhigirey, T. Day, R. Annabhimoju, W. Sherman, *J Comput Aided Mol Des* **2013**, *27*, 221-234.

[2] W. L. Jorgensen, L. Chandrasekhar, J. D. Madura, R. W. Impey, M. L. Klein, *J. Chem. Phys.* **1983**, *79*, 10.

[3] K. Lindorff-Larsen, S. Piana, K. Palmo, P. Maragakis, J. L. Klepeis, R. O. Dror, D. E. Shaw, *Proteins* **2010**, *78*, 1950-1958.

[4] O. Allner, L. Nilsson, A. Villa, *J Chem Theory Comput* **2012**, *8*, 1493-1502.

[5] K. L. Meagher, L. T. Redman, H. A. Carlson, *J.Comput.Chem.* **2003**, *24*, 1016-1025.

[6] D. A. Case, V. Babin, J. Berryman, R. M. Betz, Q. Cai, D. S. Cerutti, T. Cheatham, T. Darden, R. Duke, H. Gohlke, A. Götz, S. Gusarov, N. Homeyer, P. Janowski, J. Kaus, I. Kolossváry, A. Kovalenko, T.-S. Lee, P. A. Kollman, *AMBER 14, University of California, San Francisco*, **2014**.

[7] J. Wang, W. Wang, P. A. Kollman, D. A. Case, *J Mol Graph Model* **2006**, *25*, 247-260.

[8] S. Pronk, S. Pall, R. Schulz, P. Larsson, P. Bjelkmar, R. Apostolov, M. R. Shirts, J. C. Smith, P. M. Kasson, D. van der Spoel, B. Hess, E. Lindahl, *Bioinformatics.* **2013**, *29*, 845-854.

[9] G. Bussi, D. Donadio, M. Parrinello, *J.Chem.Phys.* **2007**, *126*, 014101.

[10] M. Parrinello, A. Rahman, *Journal of Applied Physics* **1981**, *52*, 7182-7182.

[11] B. Hess, H. Bekker, H. J. C. Berendsen, J. G. E. M. Fraaije, *J. Comput. Chem.* **1997**, *18*, 10.

[12] G. La Sala, S. Decherchi, M. De Vivo, W. Rocchia, *ACS Cent Sci* **2017**, *3*, 949-960.

[13] S. Decherchi, G. Bottegoni, A. Spitaleri, W. Rocchia, A. Cavalli, *J Chem Inf Model* **2018**, *58*, 219-224.

[14] M. L. Connolli, *J. Appl. Cryst.* **1983**, *5*, 11.

[15] aA. E. Prota, K. Bargsten, D. Zurwerra, J. J. Field, J. F. Diaz, K. H. Altmann, M. O. Steinmetz, *Science* **2013**, *339*, 587-590; bA. E. Prota, M. M. Magiera, M. Kuijpers, K. Bargsten, D. Frey, M. Wieser, R. Jaussi, C. C. Hoogenraad, R. A. Kammerer, C. Janke, M. O. Steinmetz, *J.Cell Biol.* **2013**, *200*, 259-270.

[16] J. T. Ng, C. Dekker, M. Kroemer, M. Osborne, F. von Delft, *Acta Crystallogr D Biol Crystallogr* **2014**, *70*, 2702-2718.

[17] O. B. Cox, T. Krojer, P. Collins, O. Monteiro, R. Talon, A. Bradley, O. Fedorov, J. Amin, B. D. Marsden, J. Spencer, F. von Delft, P. E. Brennan, *Chem Sci* **2016**, *7*, 2322-2330.

[18] C. Vonrhein, C. Flensburg, P. Keller, A. Sharff, O. Smart, W. Paciorek, T. Womack, G. Bricogne, *Acta Crystallogr D Biol Crystallogr* **2011**, *67*, 293-302.

[19] P. D. Adams, P. V. Afonine, G. Bunkoczi, V. B. Chen, I. W. Davis, N. Echols, J. J. Headd, L. W. Hung, G. J. Kapral, R. W. Grosse-Kunstleve, A. J. McCoy, N. W. Moriarty, R. Oeffner, R. J. Read, D. C. Richardson, J. S. Richardson, T. C. Terwilliger, P. H. Zwart, *Acta Crystallogr.D.Biol.Crystallogr.* **2010**, *66*, 213-221.

[20] P. Emsley, K. Cowtan, *Acta Crystallogr.D.Biol.Crystallogr.* **2004**, *60*, 2126-2132.

[21] I. W. Davis, L. W. Murray, J. S. Richardson, D. C. Richardson, *Nucleic Acids Res.* **2004**, *32*, W615-W619.

[22] R. B. Ravelli, B. Gigant, P. A. Curmi, I. Jourdain, S. Lachkar, A. Sobel, M. Knossow, *Nature* **2004**, *428*, 198-202.

Table S1. Tubulin pockets predicted by MD simulation.

β-Tubulin

pID [1]	Max. volume [2] (Å^3)	SS [3]	ResID [4] (p > 20 %)	Average Volume [5] (Å^3)	Persistency [6] (%)	Notes
βI	271.5	βT5 βH5 βH11	**βPro 173** (β-ns) **βSer 174** (β-ns) βPro 175 **βSer 178** (β-ns) βThr 180 βVal 181 **βGlu 183** (β-ns) βPro 184 βArg 390 βIle 391 βGln 394	111.2	58	Part of the maytansine site where the C15-C33 moiety of plocabulin binds Equivalent to pID αI
β-ns	738.5	βH1 βS4 βT4 βS5 βT5 βH5 βH6 βH7	**βGln 11** (βII) **βCys 12** (βII) **βGln 15** (βVI) βIle 16 **βSer 140** (βII) βGly 142 βVal 171 **βPro 173** (βI) **βSer 174** (βI) βVal 177 **βSer 178** (βI) **βGlu 183** (βI) βAsn 206 βLeu 209 βTyr 224 βLeu 227 βAsn 228 βVal 231	223.4	87	Occupied with GDP
βII	736.5	βS1 βH1 βS2 βT2 βS4 βT4 βH4	βAla 9 βGly 10 **βGln 11** (β-ns) **βCys 12** (β-ns) βGly 13 βAsp 69 βGlu 71 βGly 98 βAla 99 βGly 100 βAsn 101	201.4	99	γ-phosphate site of the guanosine nucleotide

			βSer 140 (β-ns) βGly 143 βGly 144 βThr 145 βGly 146			
βIII	757.9	βS4 βS5 βH5-S6 βS6 βH7 βT7 βH8 βS7 βS8 βS10	βGln 136 βIle 165 βAsn 167 βPhe 169 βAsp 199 βGlu 200 βTyr 202 βGly 237 βVal 238 βThr 239 βThr 240 βCys 241 βLeu 242 **βLeu 248** (βIV) βAsn 249 βAsp 251 βLeu 252 **βLeu 255** (βIV) βAla 256 **βMet 259** (βIV) βVal 260 βPhe 268 **βAla 316** (βIV) βIle 318 βIle 378	302.1	100	Part of the colchicine site
βIV	588.6	βT7 βH8 βS8 βH10-S9 βS9	**βLeu 248** (βIII) **βLeu 255** (βIII) βAsn 258 **βMet 259** (βIII) βThr 314 βVal 315 **βAla 316** (βIII) βIle 347 βPro 348 βAsn 349 βAsn 350 βVal 351 βLys 352	137.0	70	Part of the colchicine site Equivalent to pID αVI
βV	912.8	βH1 βS7 βM βS8 βS9-S10	**βLys 19** (βVI) βVal 23 βGly 225 βAsn 228 βHis 229	324.7	98	Part of the taxane site

		βS10	βLeu 230 βSer 232 βAla 233 βSer 236 βGly 237 βPhe 272 **βPro 274** (βXI) βLeu 275 **βThr 276** (βXI) βSer 277 βArg 278 βGly 279 βSer 280 **βGln 281** (βXI) βGln 282 βTyr 283 βArg 320 βPro 360 βArg 369 βGly 370 **βLeu 371** (βXI) βSer 374 βThr 376			
βVI	633.3	βH1 βH2 βH2-S3	**βGln 15** (β-ns) βAla 18 **βLys 19** (βV) βGlu 22 βSer 77 βVal 78 βSer 80 βPro 82 βPhe 83 βGly 84	98.8	52	Unknown pocket Mediating communication between β-ns and the taxane site Equivalent to pID αIV
βVII	230.0	βH3 βH5 βH11-H12 βH12	βTrp 103 βTyr 108 βLeu 189 βHis 192 βGln 193 βMet 413 βGlu 417 βGlu 420 βAla 421	83.4	32	Unknown pocket
βVIII	673.9	βH6 βH9-S8	βAla 208 βAsp 211 βIle 212 βArg 215 βThr 216 **βSer 298** (βX)	109.8	57	Unknown pocket

			βLys 299 **βMet 301** (βX) βAla 303 βAla 304 βCys 305			
βIX	144.1	βT2 βT3 βH3	βLeu 70 βGly 95 βGln 96 βSer 97 βGlu 110 βGlu 113 βLeu 114	78.3	31	Unknown pocket
βX	529.3	βS7 βH9 βH9-S8 βS8 βS10	βMet 269 βMet 295 βPhe 296 βAsp 297 **βSer 298** (βVIII) **βMet 301** (βVIII) βPro 307 βArg 308 βTyr 312 βPhe 377	123.6	46	Part of the laulimalide/peloruside site Equivalent to pID αXI
βXI	753.6	βM βS9-S10 βS10	**βPro 274** (βV) **βThr 276** (βV) **βGln 281** (βV) βGln 282 βTyr 283 βArg 284 βAla 285 βLeu 286 βGly 370 **βLeu 371** (βV) βLys 372 βMet 373	140.3	41	Part of the taxane site
X1	441.4	βH9-S8 βH11 βH12	βHis 309 βGly 310 βAla 383 βGln 385 βGlu 386 βGln 436 βThr 439	113.2	31	Most likely an artifact as it involves the actual C-terminus of the used β-tubulin structure

α-Tubulin

pID [1]	Max. volume [2] (Å^3)	SS [3]	ResID [4] (p > 20 %)	Average Volume [5] (Å^3)	Persistency [6] (%)	Note [7]
αI	936.0	αS5 αT5 αH5 αS6 αH6 αH9-S8 αH11	**αTyr 172** (α-ns) **αPro 173** (α-ns) **αAla 174** (α-ns) αPro 175 **αSer 178** (α-ns) **αAla 180** (α-ns) **αVal 181** (α-ns) αGlu 183 αPro 184 αSer 187 **αAsp 205** (αII) **αGlu 207** (αII) **αLys 304** (αII) **αCys 305** (αII) **αAla 387** (αII) **αArg 390** (αII) **αLeu 391** (αII) **αLys 394** (αII) αLeu 397 αMet 398	246.6	86	Unknown pocket Equivalent to pID βI Merges with pID αII
α-ns	1020.4	αH1 αS2 αT2 αH2 αT3 αS4 αT4 αH4 αS5 αT5 αH5 αH6 αH7	αGly 10 αGln 11 αAla 12 **αGln 15** (αIV) αIle 16 αAsp 69 αGlu 71 αThr 73 αVal 74 αAsp 98 αAla 99 αAla 100 αAsn 101 αSer 140 **αPhe 141** (αII) αGly 142 αGly 143 αGly 144 αThr 145 αGly 146 αIle 171 **αTyr 172** (αI) **αPro 173** (αI)	519.6	100	Occupied with GTP

			αAla 174 (αI) αVal 177 **αSer 178** (αI) αThr 179 **αAla 180** (αI) **αGlu 183** (αI) αAsn 206 **αTyr 224** (αIV) αLeu 227 **αAsn 228** (αIV) αIle 231			
αII	945.1	αT4 αS5 αS6 αH6 αH8-S7 αS7 αH9-S8 αS10-H11 αH11	**αPhe 141** (α-ns) αTyr 172 αMet 203 αVal 204 **αAsp 205** (αI) **αGlu 207** (αI) **αPhe 267** (αIII) αPro 268 **αLeu 269** (αXI) **αAla 270** (αXI) **αVal 303** (αXI) **αLys 304** (αI) **αCys 305** (αI) αAsp 306 **αPro 307** (αXI) αHis 309 αAla 383 αIle 384 αGlu 386 **αAla 387** (αI) **αTrp 388** (αIII) **αArg 390** (αI) **αLeu 391** (αI) **αLys 394** (αI)	327.7	77	Merges with pID αI
αIII	924.9	αH5 αH8-S7 αH11	αThr 191 αHis 192 αLeu 195 αGlu 196 αPro 263 αArg 264 αHis 266 **αPhe 267** (αII) **αTrp 388** (αII) αAsp 424 αLeu 428 αTyr 432	125.3	62	Unknown pocket
αIV	541.4	αH1	**αGln 15** (α-ns)	148.2	69	Unknown pocket

		αH2 αH2-S3 αH7	αAsn 18 αAla 19 **αGlu 22** (αX) αGlu 77 αVal 78 αThr 82 **αTyr 83** (αX) **αTyr 224** (α-ns) **αThr 225** (α-ns) αAsn 228 αArg 229			Equivalent to pID βVI Communicates with α-ns
αV	649.6	αM αS9-S10 αS10	**αPro 274** (αIX) **αIle 276** (αXII) αLys 280 αAla 281 αTyr 282 αHis 283 αGlu 284 αGln 285 αLeu 286 **αAla 369** (αXII) αLys 370 **αVal 371** (αXII) αGln 372 αArg 373	136.6	51	Unknown pocket Communicates with pID αXII
αVI	496.7	αH8 αH8-S7 αS8 αH10-S9 αS9	αAsn 258 αPro 261 αMet 313 αAla 314 αCys 315 αPhe 343 αCys 347 αPro 348 αGly 350 αPhe 351 αLys 352	115.4	52	Unknown pocket Equivalent to pID βIV
αVII	507.0	αH1-S2 αH2-S3 αH3	αSer 54 αGlu 55 αThr 56 αVal 62 αPro 63 αArg 64 αHis 88 αGlu 90 αGln 91 αArg 121 αLys 124 αLeu 125	154.2	85	Unknown pocket

			αGln 128			
αVIII	744.8	αH1 αH1-H1' αH7 αS8 αS9-S10	**αLeu 26** (αX) αGlu 27 αThr 41 αIle 42 αGly 43 αGly 44 αPhe 244 αArg 320 αGln 358 αPro 359 αPro 360 αThr 361 αLys 370	162.8	51	Unknown pocket
αIX	439.8	αH6 αS7 αM αH9 αH9-S8	αIle 212 αAsn 216 αTyr 272 αAla 273 **αPro 274** (αV) αVal 275 αAla 294 αAsn 300	100.9	30	Unknown pocket
αX	508.9	αH1 αH1-H1' αH2-S3 αS9-S10	**αGlu 22** (αIV) αCys 25 **αLeu 26** (αVIII) αIle 30 αGln 31 αPro 32 **αTyr 83** (αIV) αPro 364	122.8	30	Unknown pocket
αXI	689.0	αS7 αH9 αH9-S8 αS8 αS10	**αLeu 269** (αII) **αAla 270** (αII) αThr 271 αCys 295 αPhe 296 αGln 301 **αVal 303** (αII) **αPro 307** (αII) αArg 308 αTyr 312 αMet 377 αSer 379	114.6	51	Unknown pocket Equivalent to pID βX
αXII	392.5	αH7 αS7 αM αS9-S10	αGln 233 αTyr 272 αPro 274 αVal 275 **αIle 276** (αV)	80.0	32	Unknown pocket Equivalent to pID βV Communicates with pID αV

			αPro 360 αThr 361 αVal 362 αLeu 368 **αAla 369** (αV) **αVal 371** (αV)			

[1]Pocket identifiers. ns, nucleotide site.
[2]Maximal pocket volume during the simulation.
[3]Secondary structural elements involved in pocket formation.
[4]Residues involved in pocket formation in >20 % of the time during the simulation. Residues involved in a pocket communication network are highlighted in bold; the adjacent pocket that shares the same residue is given in parenthesis.
[5]Average pocket volume during the simulation.
[6]Persistency of the pocket during the simulation.

Table S3. Tubulin fragment-binding sites identified by X-ray crystallography.

β-Tubulin

sID [1]	SS [2]	ResID [3]	Fragment ID [4]	V_f [5] (Å^3)	PDB ID [6]	Notes
βI	βH6 βH9 βH9-βS8	βAsp 211 βIle 212 βArg 215 βThr 216 βLys 218 βSer 298 βLys 299	01 53	173	5S4L 5S61	Unknown ligand-binding site Residue substitutions in human β-tubulin isotypes: β2a/β2b, A298S; β1/β6, K299R; β8, R215K
βII	βH1 βH7 βS7 βM βS8 βS9-βS10 βS10	βVal 23 βGlu 27 βHis 229 βAla 233 βThr 234 βSer 236 βGly 237 βPhe 272 βPro 274 βArg 320 βPro 360 βArg 369 βLeu 371 βSer 374 βThr 376	02 03	207	5S4M 5S4N	Taxane site Residue substitutions in human β-tubulin isotypes: β1, V23M, A233L, A374S; β4a/β5/β6, S374A
βIII	βN-ter βH1' βT7	αThr 73 βMet 1 βLeu 46 βGlu 47 βArg 48 βIle 49 βAsn 50 βVal 51 βAla 250 βAsp 251	04	179	5S4O	Unknown ligand-binding site Residue substitutions in human β-tubulin isotypes: β5, E47D, N50S
βIV	αT5 βS1 βH1' βS4 βS5 βS6 βH7 βT7 βH8	αThr 179 αAla 180 αVal 181 βIle 4 βTyr 52 βGln 136 βAsn 167 βPhe 169 βGlu 200	03 05 06 07 08 09 10 11 12	780	5S4N 5S4P 5S4Q 5S4R 5S4S 5S4T 5S4U 5S4V 5S4W	Colchicine site Residue substitutions in human β-tubulin isotypes: β1, E200A, Y202F, V238I, C241S, A317C, V318I, T353V; β2a/β2b, V318I; β3/β6, C241S, A317T, T353V; β8, Y202F, V318I

	βS8 βS9 βS10	βTyr 202 βVal 238 βThr 239 βCys 241 βLeu 242 βGln 247 βLeu 248 βAsn 249 βAla 250 βLeu 252 βLeu 255 βAla 256 βAsn 258 βMet 259 βPhe 268 βAla 316 βAla 317 βIle 318 βAsn 350 βLys 352 βThr 353 βAla 354 βIle 378	13 14 15 16 17 18 19		5S4X 5S4Y 5S4Z 5S50 5S51 5S52 5S53	
βV	αH11' βS4 βH4 βH4-βS5 βS5 βH5 βH5-βS6 βH8 βH8-βS7	αHis 406 αVal 409 αGly 410 αGlu 411 βPhe 135 βIle 154 βIle 157 βArg 158 βTyr 161 βPro 162 βAsp 163 βArg 164 βIle 165 βMet 166 βVal 195 βGlu 196 βAsn 197 βThr 198 βAsp 199 βArg 253 βPro 263 βArg 264 βHis 266	14 20 21 22 23 24 25 26	669	5S4Y 5S54 5S55 5S56 5S57 5S58 5S59 5S5A	Unknown ligand-binding site Residue substitutions in human β-tubulin isotypes: β1, I154L, V195I, T198A; β3, I157V; β4a/β6, Y161F; β8, I154M, M166I, V195I, T198A

β1α2-Tubulin

sID [1]	SS [2]	ResID [3]	Fragment ID [4]	V_f [5] (Å^3)	PDB ID [6]	Notes
βαI	αH8-αS7 αH12 βH11-βH11'	αTyr 262 αPro 263 αArg 264 αIle 265 αAsp 431 αGlu 434 αVal 435 βArg 400 βArg 401 βLys 402	27 28 29	511	5S5B 5S5C 5S5D	Unknown ligand-binding site Residue substitution in human β-tubulin isotypes: β1, R400K
βαII	αH3-S4 αS4 αH4-αS5 αS6 αH8 βT3 βH3' βT5 βH11'	αCys 4 αGln 133 αGly 134 αPhe 135 αLeu 136 αSer 165 αLeu 167 αAsp 199 αCys 200 αPhe 202 αLeu 242 αLeu 252 αThr 253 αGln 256 αThr 257 αLeu 259 βGly 100 βAsn 101 βAsn 102 βLys 105 βVal 182 βTrp 407 βTyr 408 βGlu 411	04 11 30 31 32 33 34 35 36 37 38 39 40 41 42 43	632	5S4O 5S4V 5S5E 5S5F 5S5G 5S5H 5S5I 5S5J 5S5K 5S5L 5S5M 5S5N 5S5O 5S5P 5S5Q 5S5R	Unknown ligand-binding site Located between the maytansine and pironetin sites Residue substitution in human β-tubulin isotypes: β6, Y408F
βαIII	αT7 αH8 αH10 αH10-αS9 αS9 βT5 βH5 βH6 βH6-βH7 βH7	αLeu 248 αVal 250 αAsn 258 αPro 325 αVal 328 αAsn 329 αIle 332 αPro 348 αGly 350 αPhe 351	03 05 07 15 22 26 29 30 38 44	1139	5S4N 5S4P 5S4R 5S4Z 5S56 5S5A 5S5D 5S5E 5S5M 5S5S	Vinblastine site Residue substitution in human β-tubulin isotypes: β1, Q394H

	βH11	αLys 352 αVal 353 αGly 354 αIle 355 βPro 173 βSer 174 βPro 175 βLys 176 βVal 177 βSer 178 βAsp 179 βThr 180 βVal 181 βGlu 183 βPro 184 βTyr 210 βThr 221 βPro 222 βThr 223 βTyr 224 βLeu 227 βGln 394	45 46 47 48 49 50 51 52 53 54 55 56		5S5T 5S5U 5S5V 5S5W 5S5X 5S5Y 5S5Z 5S60 5S61 5S62 5S63 5S64	

α-Tubulin

sID [1]	SS [2]	ResID [3]	Fragment ID [4]	V_f [5] (Å^3)	PDB ID [6]	Notes
αI	αH6 αM αH9	αArg 215 αAsn 216 αPro 274 αVal 275 αLys 280 αLeu 286 αAla 294	05	185	5S4P	Unknown ligand-binding site Residue substitutions in human α-tubulin isotypes: α8, V275I, A294S
αII	αH1 αH2 αH2-αS3 αH7	αGln 15 αAsn 18 αAla 19 αTrp 21 αGlu 22 αGlu 77 αVal 78 αGly 81 αThr 82 αTyr 83 αPhe 87	02 25 53	364	5S4M 5S59 5S61	Unknown ligand-binding site Residue substitutions in human α-tubulin isotypes: α4a, V78I, T82P

		αThr 225 αAsn 228 αArg 229				

Crystal contact/binding partner of T_2R-TTL

sID [1]	SS [2]	ResID [3]	Fragment ID [4]	V_f [5] (Å^3)	PDB ID [6]	Notes
X1	αH1-αS2	αThr 41 αIle 42 αGly 43 αGly 44 αGly 45 αAsp 46	26 39 57	-	5S5A 5S5N 5S65	Site involving a crystal contact formed by a neighboring α-tubulin monomer
X2	αH2- αS3 αH3	αHis 88 αGlu 90 αGln 91 αArg 121 αLys 124 αLeu 125	05	-	5S4P	Site involving a crystal contact formed by a neighboring TTL molecule
X3	αH4-αS5 αH5 βH11’	αSer 158 αGly 162 αLys 163 αLys 166 αGlu 196 αHis 197 αSer 198 αAsp 199 βGly 410	58 59	-	5S66 5S67	Site involving residues of RB3

[1]Fragment site identifiers. X1, X2 and X3 refer to sites that involve either a crystal contact (X1 and X2) or a tubulin-binding partner of the T_2R-TTL complex (X3).
[2]Secondary structural elements involved in site formation.
[3]Residues that are in contact with the identified fragments (maximal distance of 4 Å).
[4]Fragment ID according to the deposited structures in the RCSB Protein Data Bank.
[5]Total fragment volume.
[6]PDB IDs for the deposited structures in the RCSB Protein Data Bank.

Table S4. Contact points of tubulin dimers in the microtubule lattice that overlap with predicted pockets or fragment sites.

β1α2-Tubulin

pID/sID [1]	ResID [2]	Secondary structural elements involved [3]
sID βαII$^{\alpha}$	αCys 4 αGln 133 αGly 134 αPhe 135 αLeu 136 αSer 165 αLeu 167 αAsp 199 αCys 200 αPhe 202 αLeu 242 αLeu 252 **αThr 253** ***αGln 256*** ***αThr 257*** αLeu 259	βT3 and βH3' (longitudinal inter-tubulin dimer contact in microtubules)
---	---	---
sID βαII$^{\beta}$	**βGly 100** ***βAsn 101*** βAsn 102 βLys 105 **βVal 182** ***βTrp 407*** βTyr 408 βGlu 411	αH8 (longitudinal inter-tubulin dimer contact in microtubules)
sID βαIII$^{\alpha}$	**αLeu 248** αVal 250 ***αAsn 258*** **αPro 325** **αVal 328** **αAsn 329** αIle 332 ***αPro 348*** **αGly 350** **αPhe 351** ***αLys 352*** **αVal 353** αGly 354 αIle 355	βT5 (longitudinal inter-tubulin dimer contact in microtubules)
---	---	---

sID $\beta\alpha III^{\beta}$	βPro 173 βSer 174 βPro 175 **βLys 176** **βVal 177** **βSer 178** ***βAsp 179*** ***βThr 180*** ***βVal 181*** βGlu 183 **βPro 184** βTyr 210 ***βThr 221*** **βPro 222** βThr 223 **βTyr 224** βLeu 227 βGln 394	αH10, αH10-αS9 loop, and αS9 (longitudinal inter-tubulin dimer contact in microtubules)

α-Tubulin

pID/sID [1]	ResID [2]	Secondary structural elements involved [3]
pID αI	αTyr 172 αPro 173 αAla 174 **αPro 175** **αSer 178** **αAla 180** **αVal 181** **αGlu 183** αPro 184 αSer 187 αAsp 205 **αGlu 207** αLys 304 αCys 305 αAla 387 αArg 390 αLeu 391 **αLys 394** **αLeu 397** **αMet 398**	βH10-βS9 loop (longitudinal intra-tubulin dimer contact)
pID αVII	**αSer 54** **αGlu 55** **αThr 56**	Adjacent αM-loop (lateral inter-tubulin dimer contact in microtubules)

	αVal 62 αPro 63 αArg 64 **αHis 88** **αGlu 90** αGln 91 **αArg 121** **αLys 124** αLeu 125 **αGln 128**	

[1]Pocket and site identifiers. Fragment sites that are located at the βTub1-αTub2 inter-dimer interface in the T_2R-TTL complex and thus represent composite sites are considered separately as half sites; they are indicated with "α" and "β" superscripts to denote whether they belong to α- or β-tubulin, respectively.

[2]Tubulin residues that are involved in pocket or site formation (taken from Table S1 and Table S3). Residues that are shared between a pocket or a site and an adjacent tubulin chain within the tubulin dimer or in the microtubule lattice (maximal distance of 4 Å) are shown in italic for unassembled "curved" tubulin and in bold for assembled "straight" tubulin. Residues that are shared between a pocket or a site independent of the conformational state of tubulin are shown in both bold and italic.

[3]Secondary structural elements of the contacting tubulin monomer involved in interaction with residues forming a pocket or a site.

The Protein Data Bank ID of the microtubule structure that was used for the analysis is PDB ID 3JAR.

Table S5. Contact points of protein partners that overlap with predicted pockets or fragment sites in tubulin.

β-Tubulin

sID/pID [1]	ResID [2]	Protein [3]	Structural element involved [4]
sID βI	βAsp 211 βIle 212 **βArg 215** βThr 216 **βSer 298** **βLys 299**	Targeting protein for Xklp2 (TPX2) PDB ID: 6BJC	C-terminal unstructured part of the wedge domain Binds also to sID βαI
sID βV	**αHis 406** **αVal 409** **αGly 410** **αGlu 411** βPhe 135 βIle 154 βIle 157 **βArg 158** βTyr 161 **βPro 162** **βAsp 163** βArg 164 βIle 165 βMet 166 **βVal 195** **βGlu 196** **βAsn 197** βThr 198 **βAsp 199** βArg 253 **βPro 263** **βArg 264** **βHis 266**	Cytoplasmic dynein 1 heavy chain PDB ID: 3J1U, 3J1T, 6RZA, 6RZB	Helix 1 of the microtubule-binding domain
sID βV	*αHis 406* *αVal 409* *αGly 410* αGlu 411 βPhe 135 βIle 154 βIle 157 *βArg 158* βTyr 161 βPro 162 βAsp 163 βArg 164	Centrosomal P4.1-associated protein (CPAP/SAS-4) PDB ID: 5ITZ, 5EIB	Helical SAC region of the N-terminal PN2-3 domain

	βIle 165 βMet 166 βVal 195 *βGlu 196* βAsn 197 βThr 198 βAsp 199 βArg 253 *βPro 263* βArg 264 βHis 266		

β1α2-Tubulin

sID/pID [1]	ResID [2]	Protein [3]	Structural element involved [4]
sID βαI	*αTyr 262* αPro 263 αArg 264 αIle 265 *αAsp 431* *αGlu 434* *αVal 435* βArg 400 *βArg 401* *βLys 402*	Kinesin-13 PDB ID: 5MIO, 6BBN, 6B0I	L2 hairpin specific to the motor domain of kinesin-13 family members
sID βαI	*αTyr 262* αPro 263 *αArg 264* αIle 265 αAsp 431 αGlu 434 αVal 435 βArg 400 βArg 401 βLys 402	Kinesin-5 PDB ID: 5MM7	Loop L2 of the motor domain of *Ustilago maydis* kinesin-5
sID βαI	**αTyr 262** **αPro 263** αArg 264 αIle 265 **αAsp 431** **αGlu 434** αVal 435 **βArg 400** **βArg 401** **βLys 402**	Targeting protein for Xklp2 (TPX2) PDB ID: 6BJC	N-terminal unstructured part of the ridge domain Binds also to sID βI

sID βαI	αTyr 262 αPro 263 **αArg 264** αIle 265 **αAsp 431** **αGlu 434** **αVal 435** **βArg 400** **βArg 401** **βLys 402**	Tau PDB ID: 6CVN, 6CVJ	R1 and R2 repeats
sID βαI$^{\alpha}$	*αTyr 262* *αPro 263* αArg 264 αIle 265 *αAsp 431* αGlu 434 *αVal 435*	iE5 alphaRep PDB ID: 6GWC	Helix 2 of the N-cap
sID βαIII$^{\alpha}$	*αLeu 248* *αVal 250* *αAsn 258* *αPro 325* αVal 328 *αAsn 329* αIle 332 *αPro 348* *αGly 350* *αPhe 351* *αLys 352* *αVal 353* *αGly 354* *αIle 355*	Stathmin like domain of RB3 PDB ID: 1FFX, 6GVM	N-terminal β-hairpin
sID βαIII$^{\beta}$	βPro 173 βSer 174 *βPro 175* *βLys 176* βVal 177 βSer 178 βAsp 179 βThr 180 *βVal 181* βGlu 183 βPro 184 βTyr 210 βThr 221 βPro 222 βThr 223 βTyr 224 βLeu 227	Designed Ankyrin Repeat Protein (DARPin) PDB ID: 4DRX, 5EYP	Repeat 4

	βGln 394		

α-Tubulin

sID/pID [1]	ResID [2]	Protein [3]	Structural element involved [4]
pID αII (αI)	αPhe 141 αTyr 172 αMet 203 αVal 204 αAsp 205 *αGlu 207* αPhe 267 αPro 268 αLeu 269 αAla 270 αVal 303 *αLys 304* αCys 305 *αAsp 306* αPro 307 *αHis 309* αAla 383 αIle 384 *αGlu 386* αAla 387 αTrp 388 *αArg 390* αLeu 391 αLys 394	Tubulin Tyrosine Ligase (TTL) PDB ID: 4IHJ	Loops β3-β4 and α9-β13
pID αV	αPro 274 αIle 276 αLys 280 *αAla 281* *αTyr 282* αHis 283 αGlu 284 *αGln 285* αLeu 286 αAla 369 *αLys 370* *αVal 371* *αGln 372* *αArg 373*	Stu2p/Alp14p PDB ID: 6MZG	Helix HRA4 of the tumor overexpressed gene 1 (TOG1) domain
pID αVI	αAsn 258 αPro 261	Stathmin like domain of RB3	N-terminal β-hairpin

	αMet 313 αAla 314 αCys 315 αPhe 343 *αCys 347* *αPro 348* *αGly 350* *αPhe 351* *αLys 352*	PDB ID: 1FFX, 6GVM	
pID αVII	αSer 54 *αGlu 55* *αThr 56* *αVal 62* αPro 63 αArg 64 *αHis 88* *αGlu 90* αGln 91 αArg 121 *αLys 124* αLeu 125 *αGln 128*	iiiA5 alphaRep PDB ID: 6GX7	Helices 2 and 4

[1]Pocket and site identifiers. Fragment sites that are located at the βTub1-αTub2 inter-dimer interface in the T_2R-TTL complex and thus represent composite sites are considered separately as half sites; they are indicated with "α" and "β" superscripts to denote whether they belong to α- or β-tubulin, respectively.

[2]Tubulin residues that are involved in pocket or site formation (taken from Table S1 and Table S3). Residues that are shared between a pocket or a site and the tubulin-binding region of a protein partner (maximal distance of 4 Å) are shown in italic for unassembled "curved" tubulin and in bold for assembled "straight" tubulin.

[3]Protein partners that target a pocket or a site. The Protein Data Bank IDs of the structures that were used for the analysis are indicated. For some proteins, the composite fragment sites located at the βTub1-αTub2 inter-dimer interface were split and considered separately as sub β-tubulin and sub α-tubulin sites (indicated with superscripts).

[4]Structural elements of the protein partner that is involved in the interaction with a pocket or a site.

Figure S1

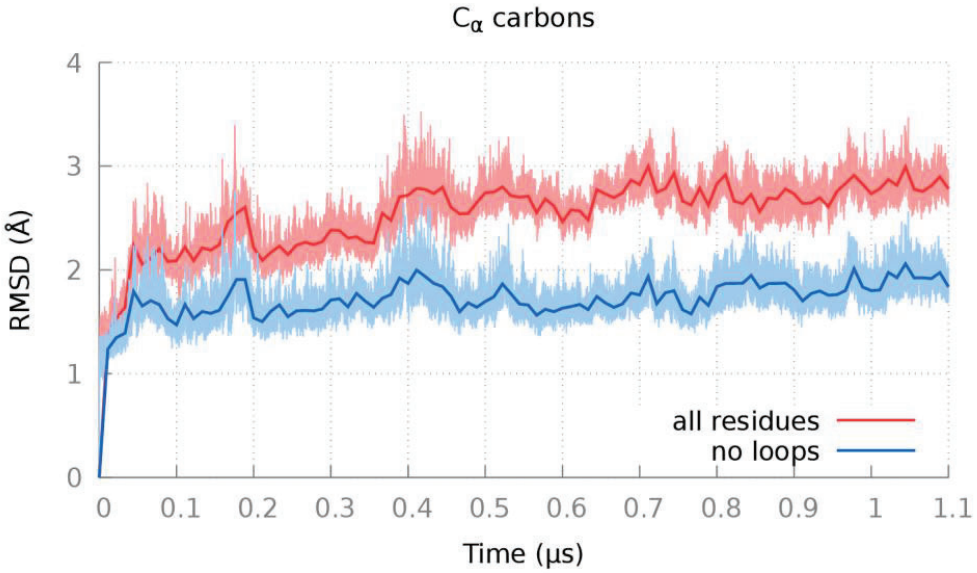
Cα carbons
RMSD (Å)
Time (μs)
all residues
no loops
0
1
2
3
4
0
0.1
0.2
0.3
0.4
0.5
0.6
0.7
0.8
0.9
1
1.1

Figure S2

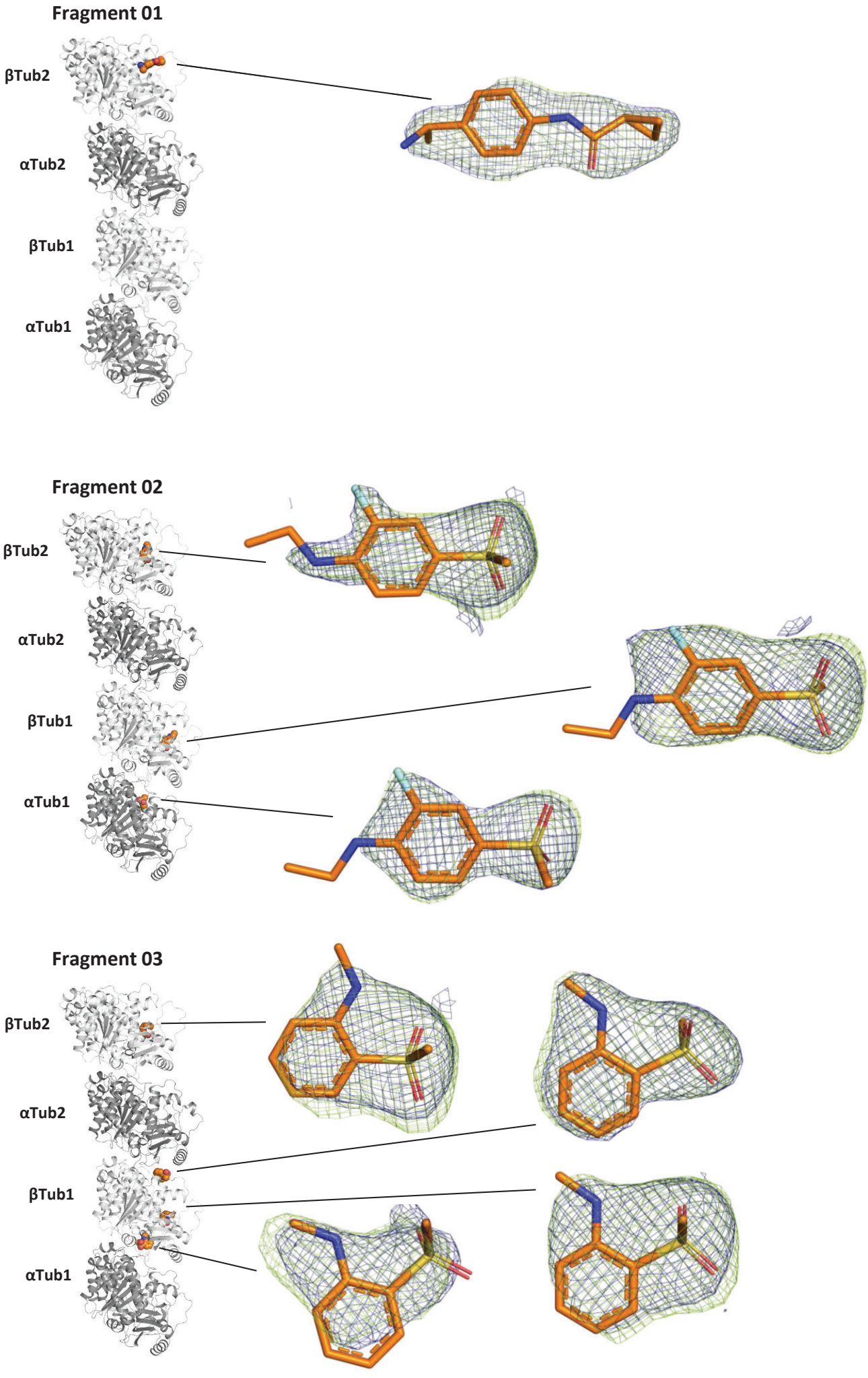
Fragment 01
βTub2
αTub2
βTub1
αTub1
Fragment 02
βTub2
αTub2
βTub1
αTub1
Fragment 03
βTub2
αTub2
βTub1
αTub1

Figure S2 (continued)

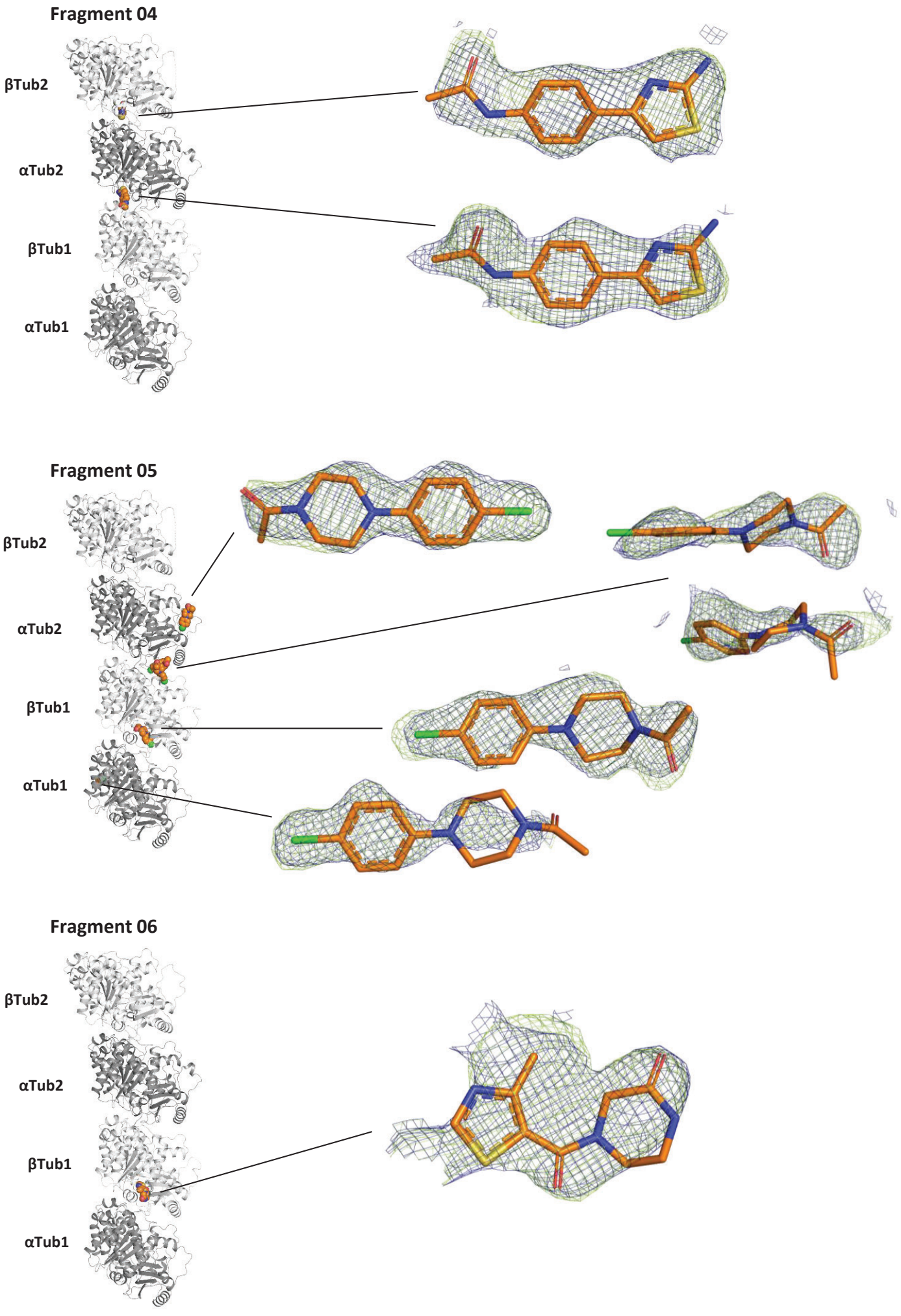

Figure S2 (continued)

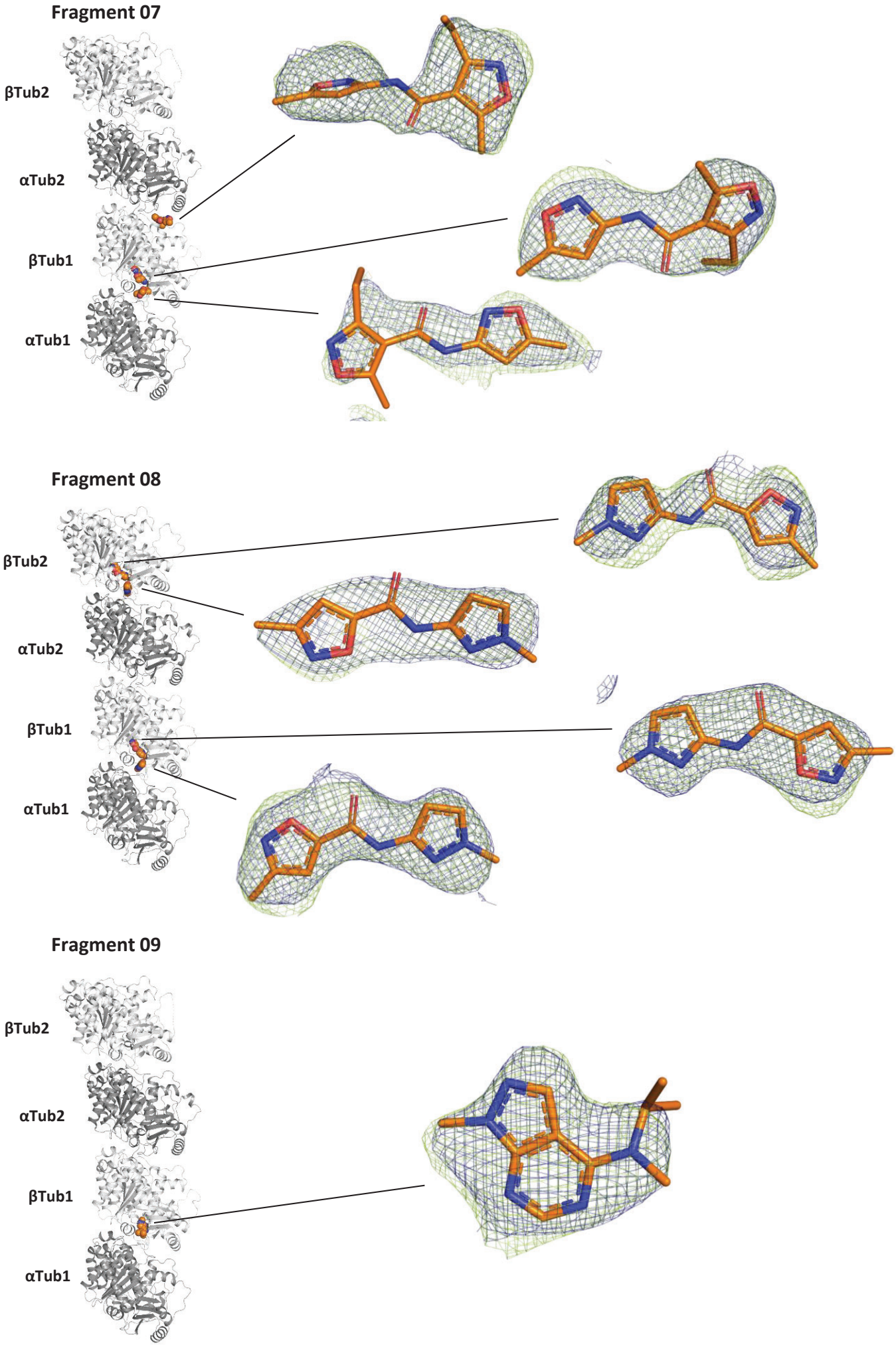

Figure S2 (continued)

Fragment 10

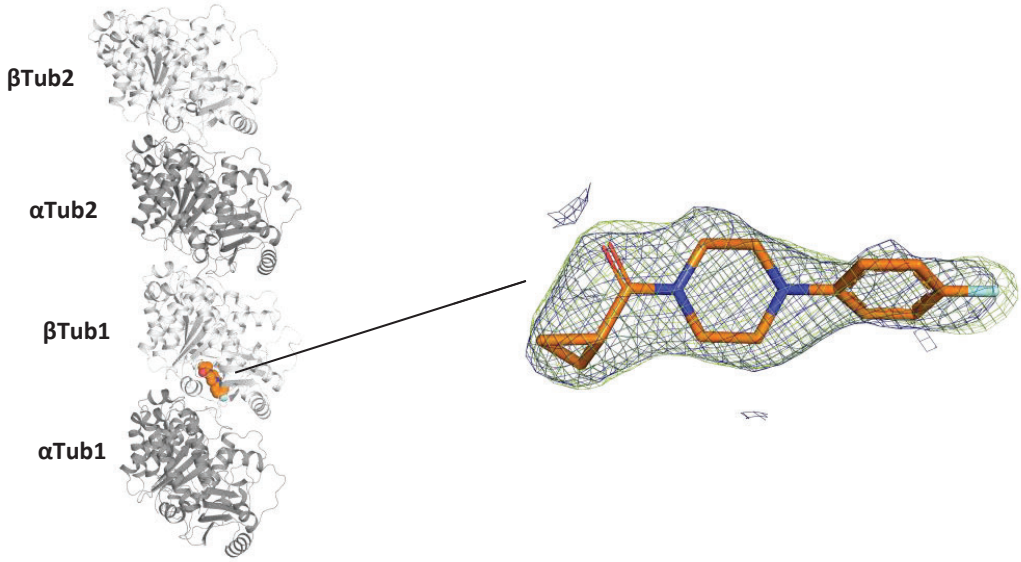

Fragment 11

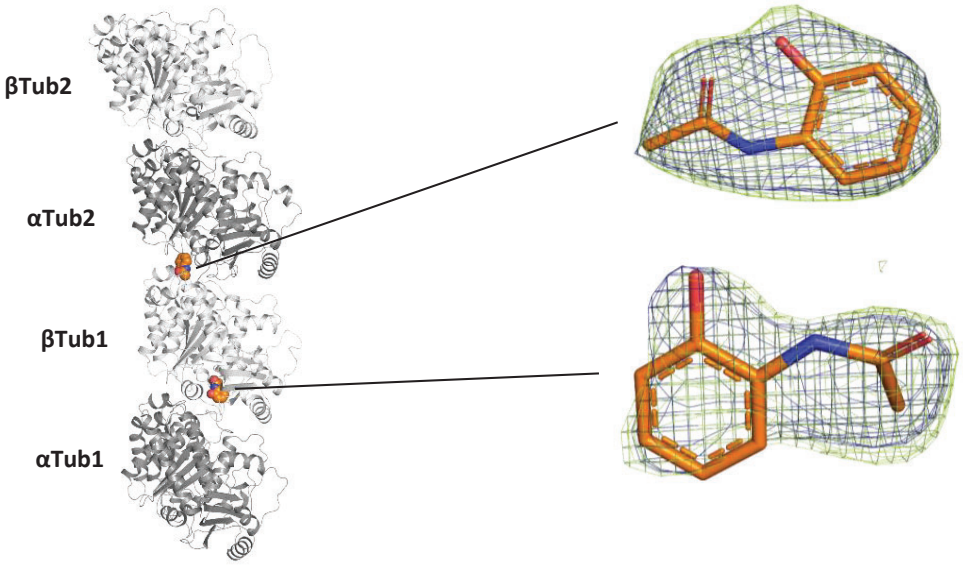

Fragment 12

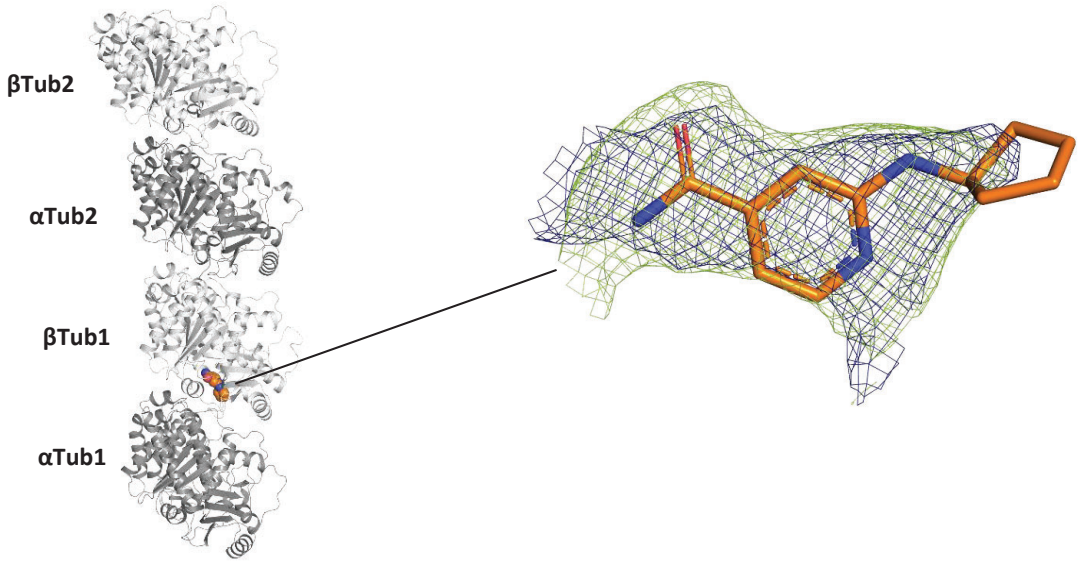

Figure S2 (continued)

Fragment 13

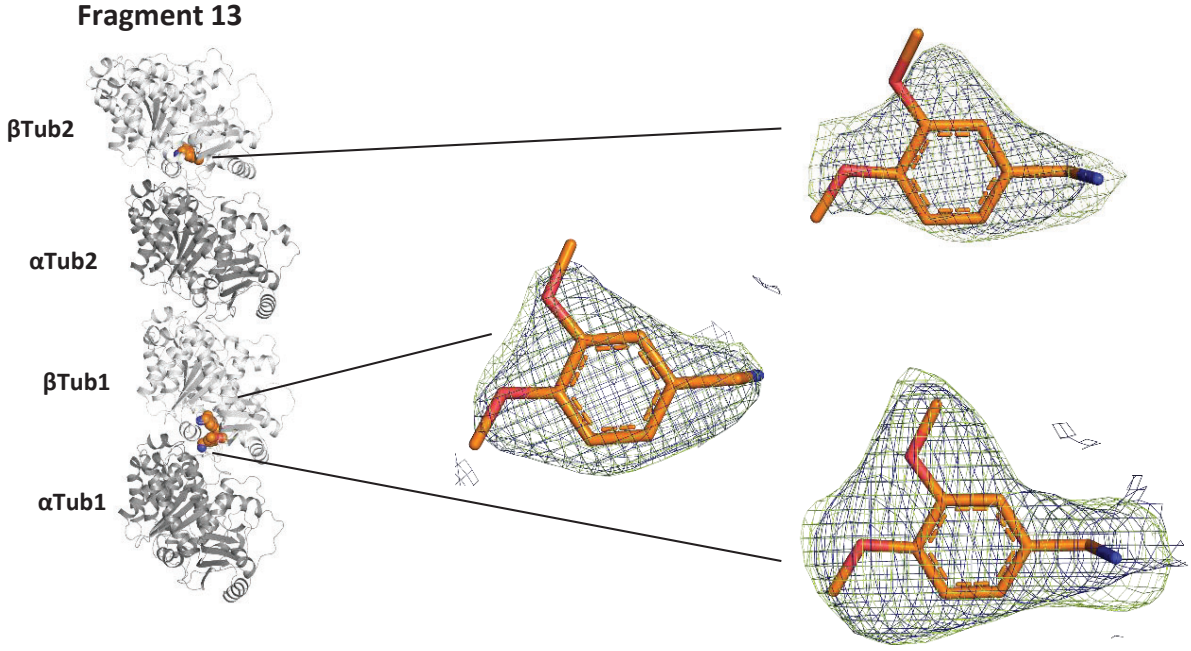

Fragment 14

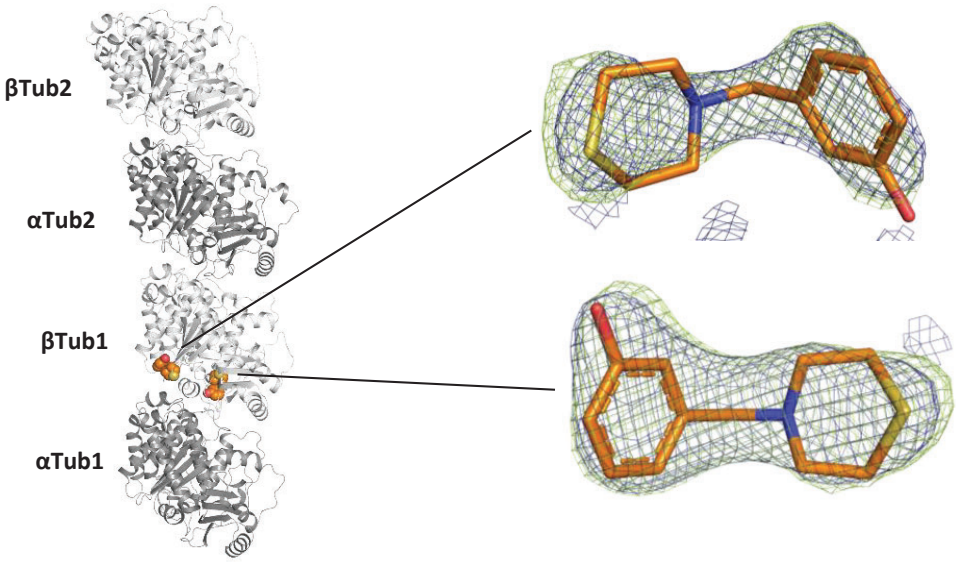

Fragment 15

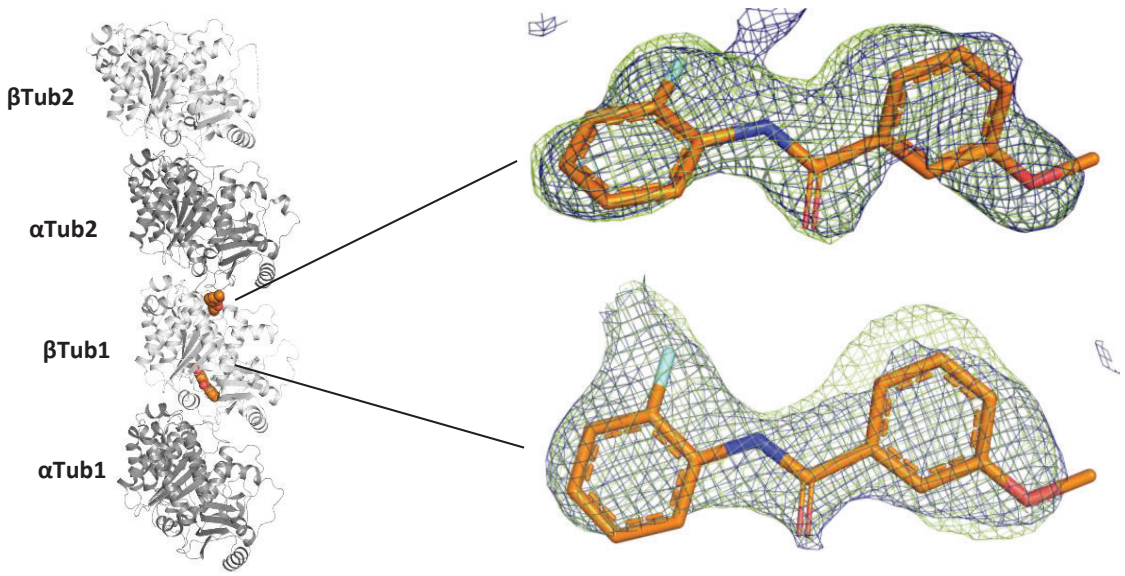

Figure S2 (continued)

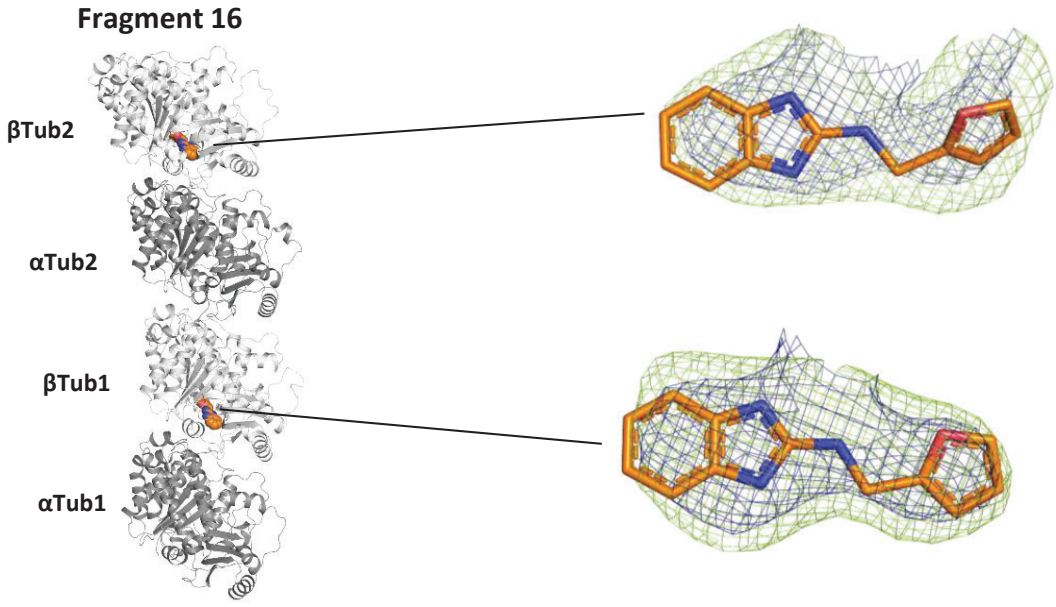

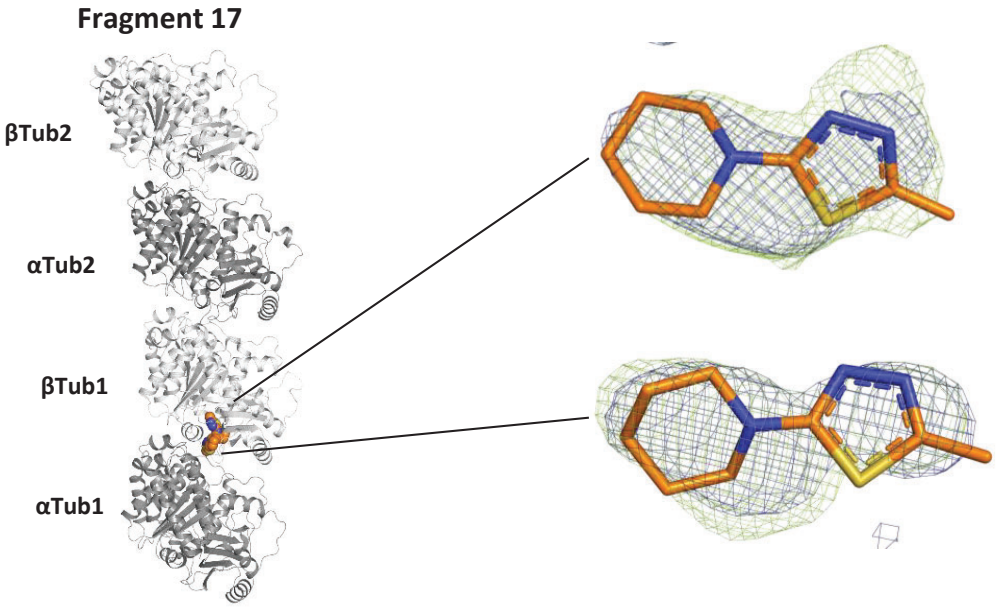

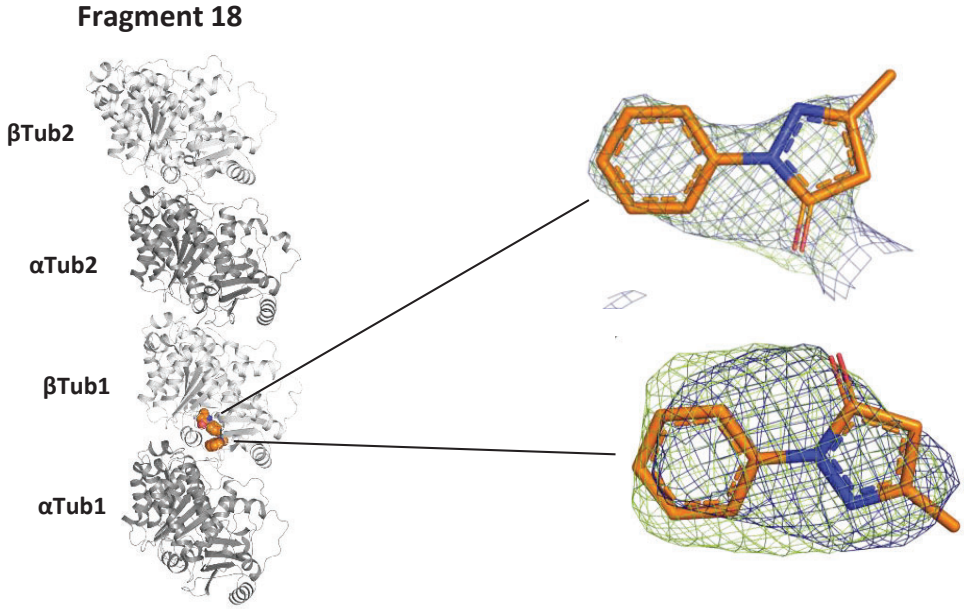

Figure S2 (continued)

Fragment 19

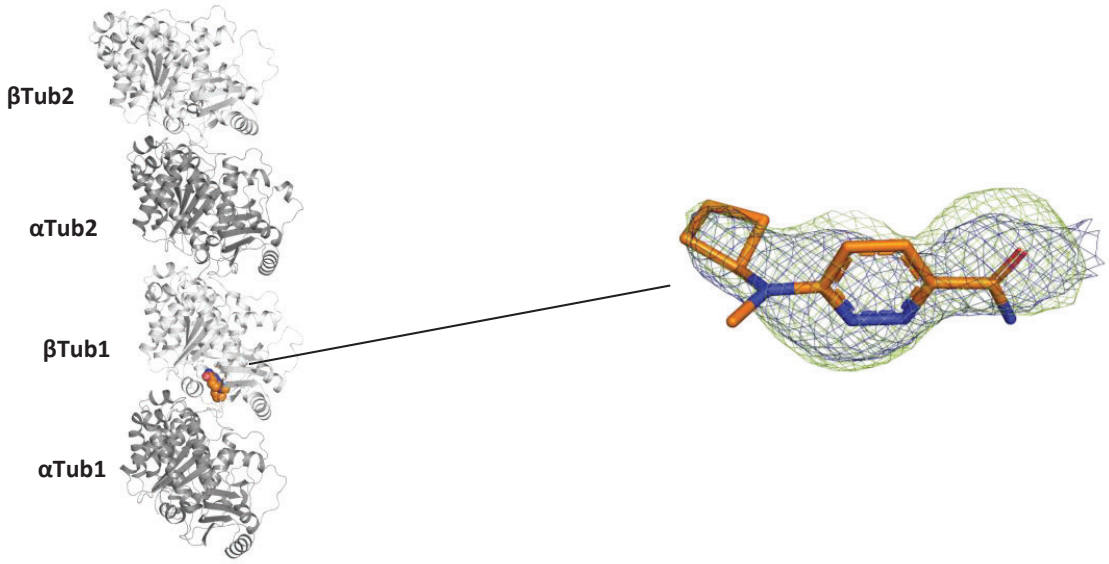

Fragment 20

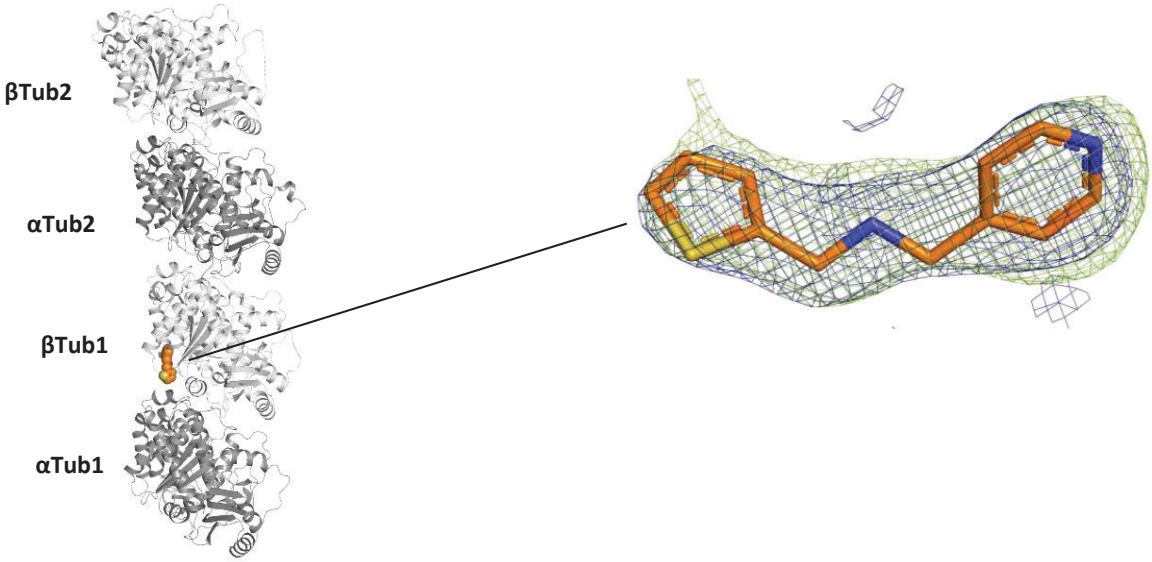

Fragment 21

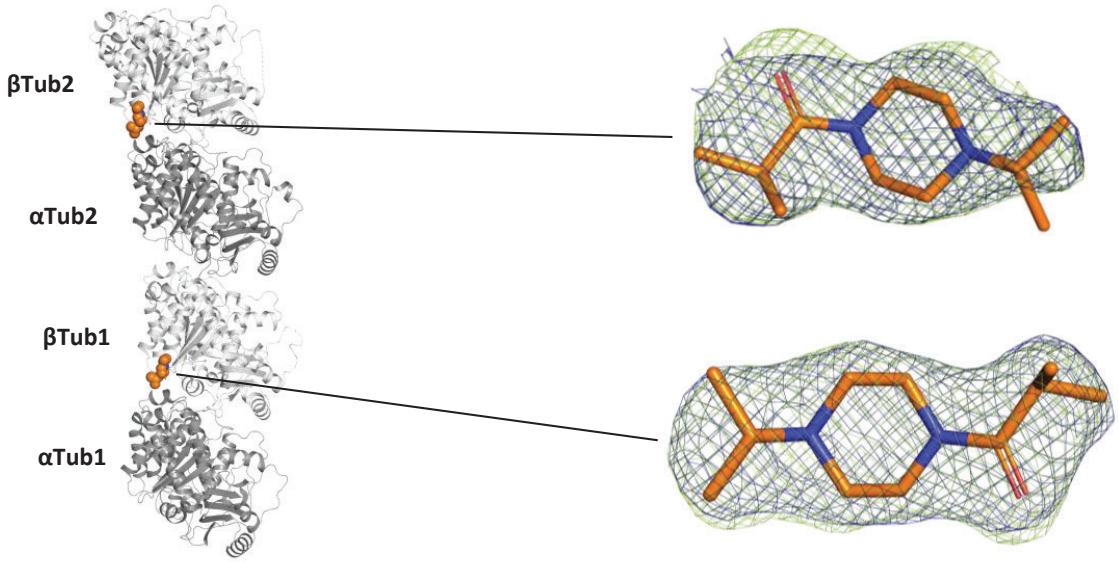

Figure S2 (continued)

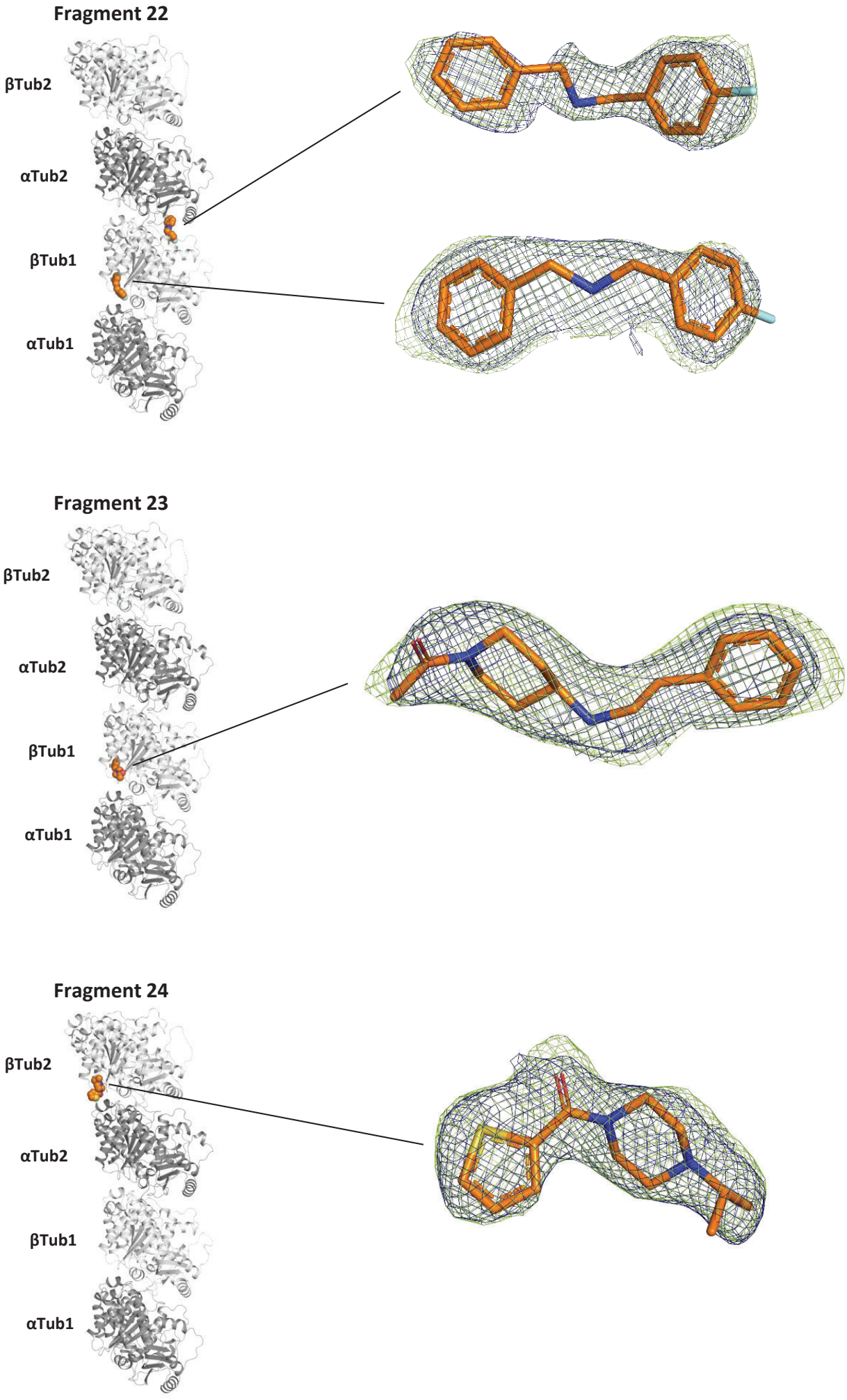

Figure S2 (continued)

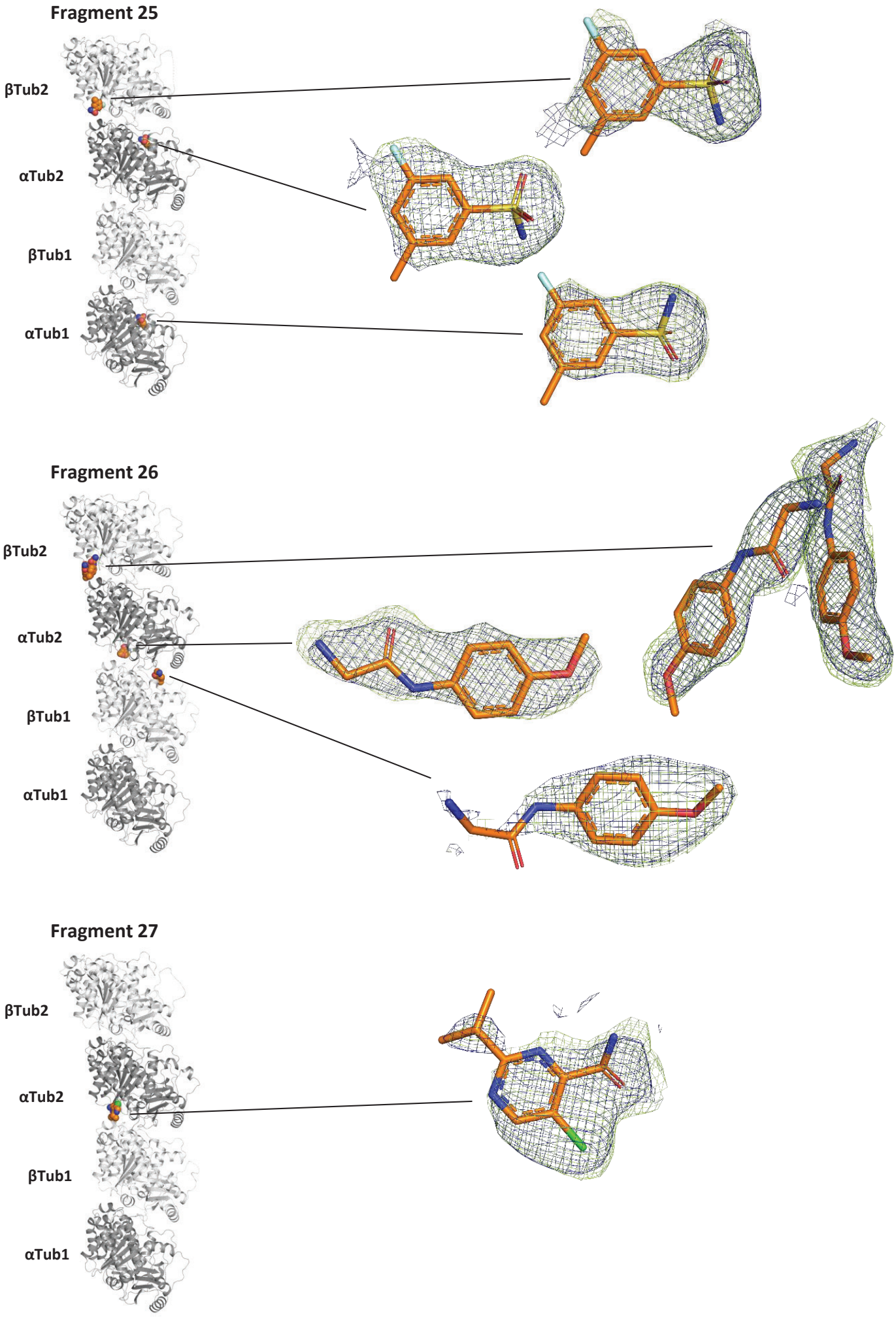

Figure S2 (continued)

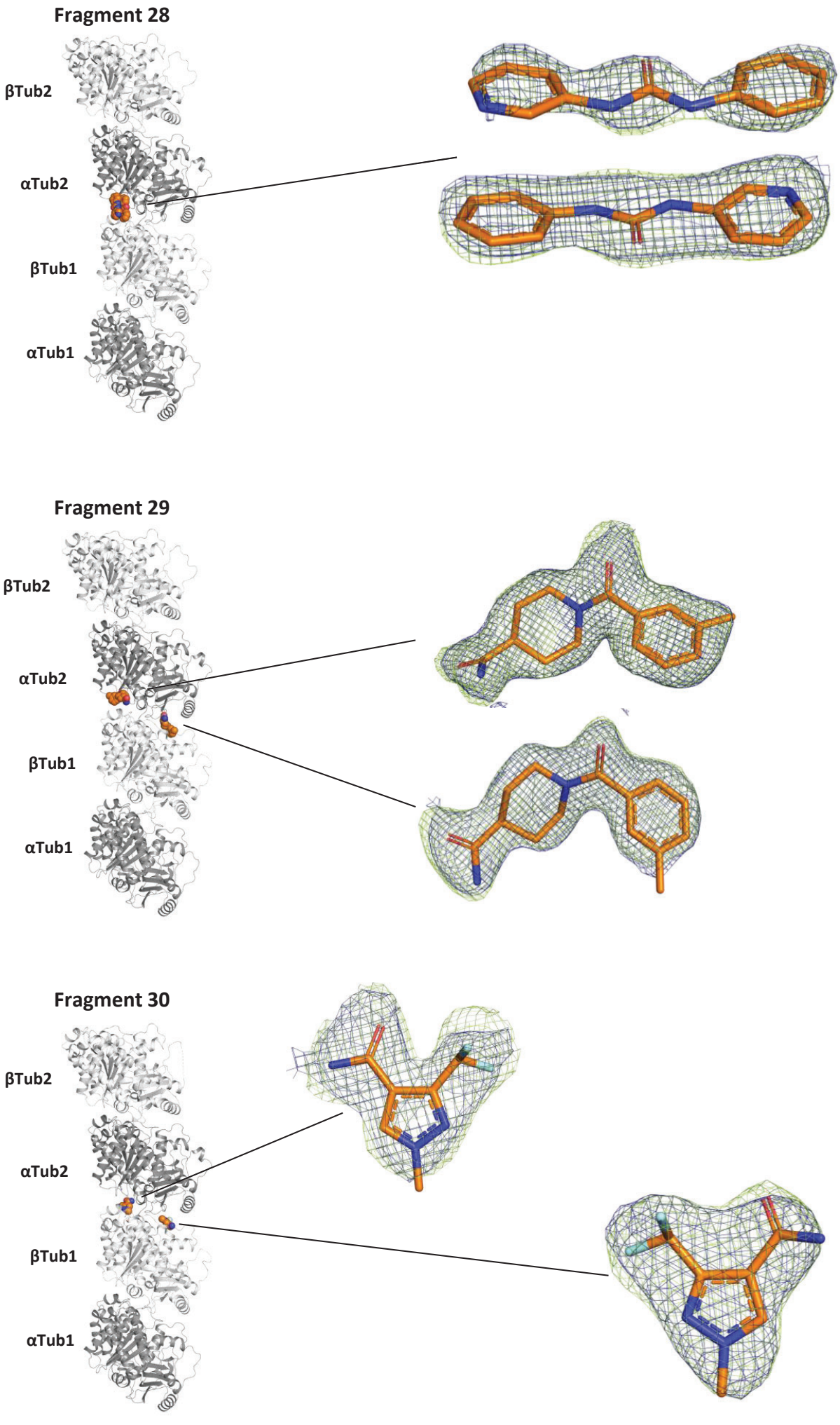

Figure S2 (continued)

Fragment 31

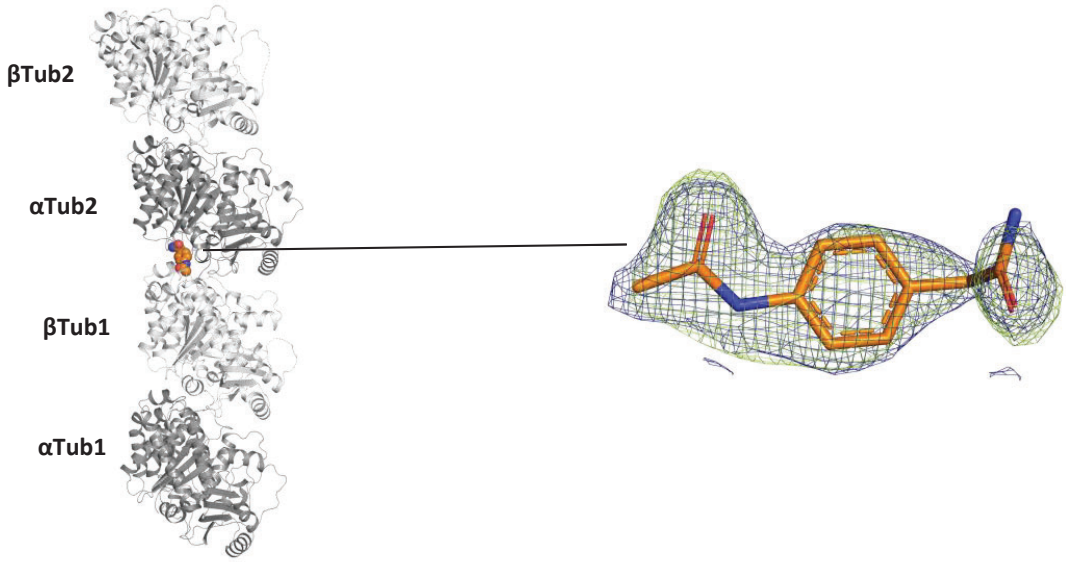

Fragment 32

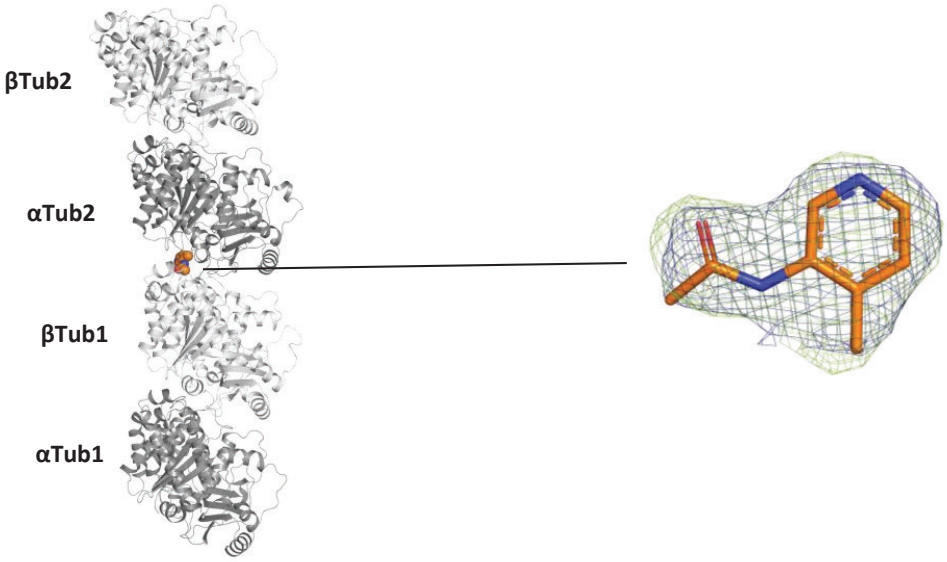

Fragment 33

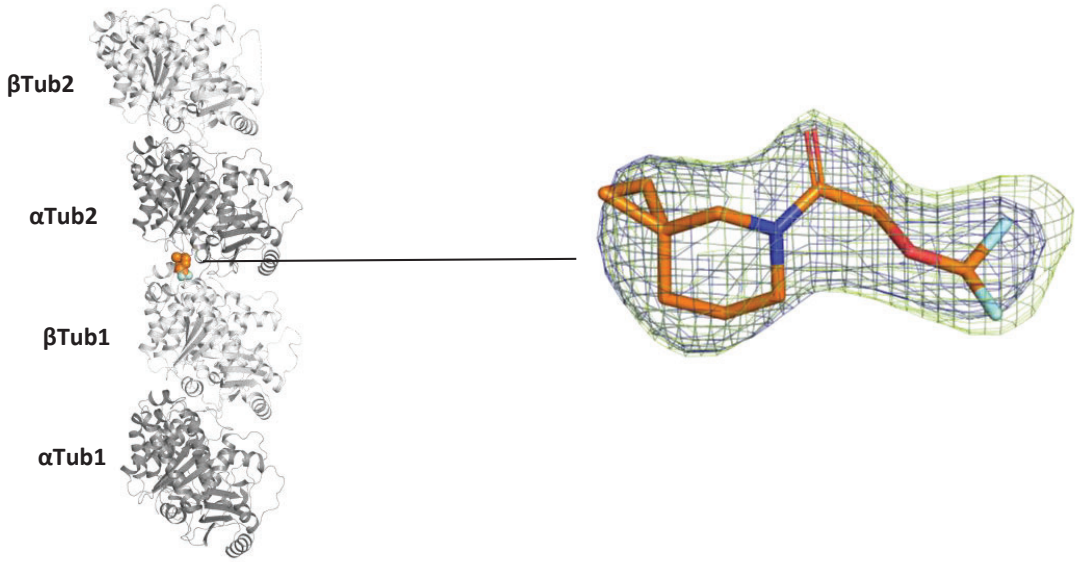

Figure S2 (continued)

Fragment 34

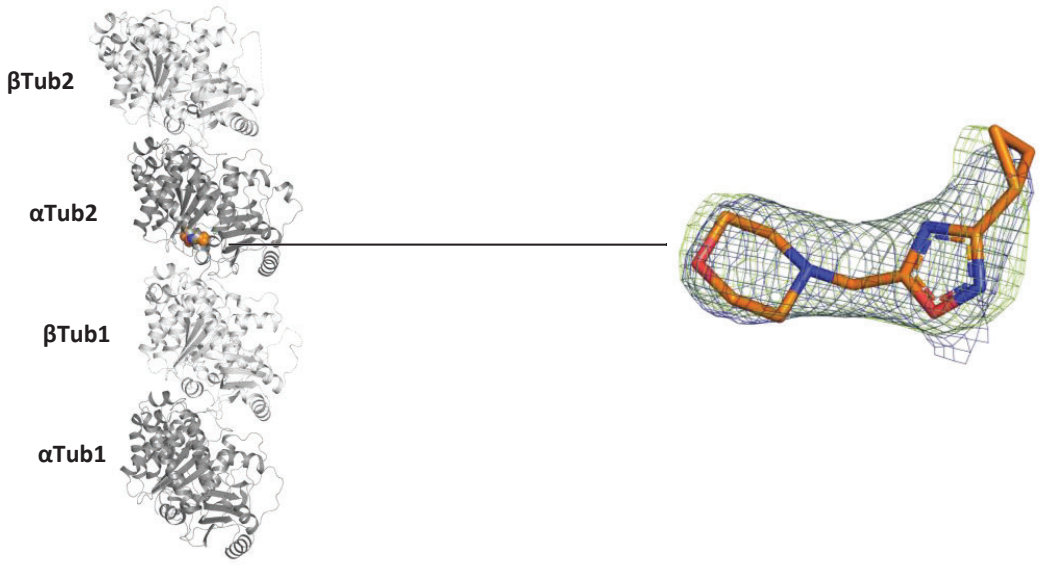

Fragment 35

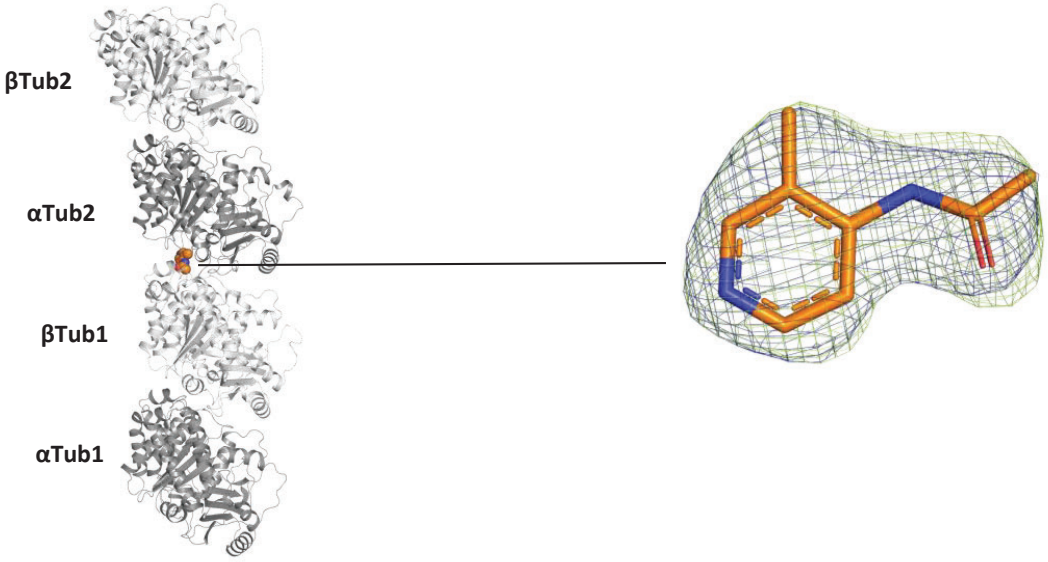

Fragment 36

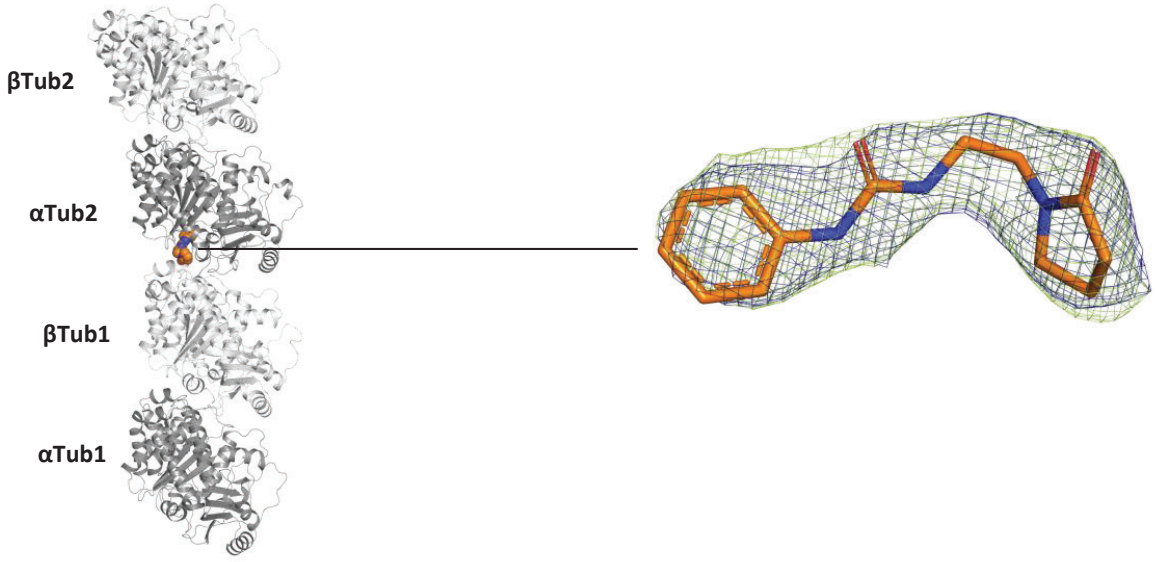

Figure S2 (continued)

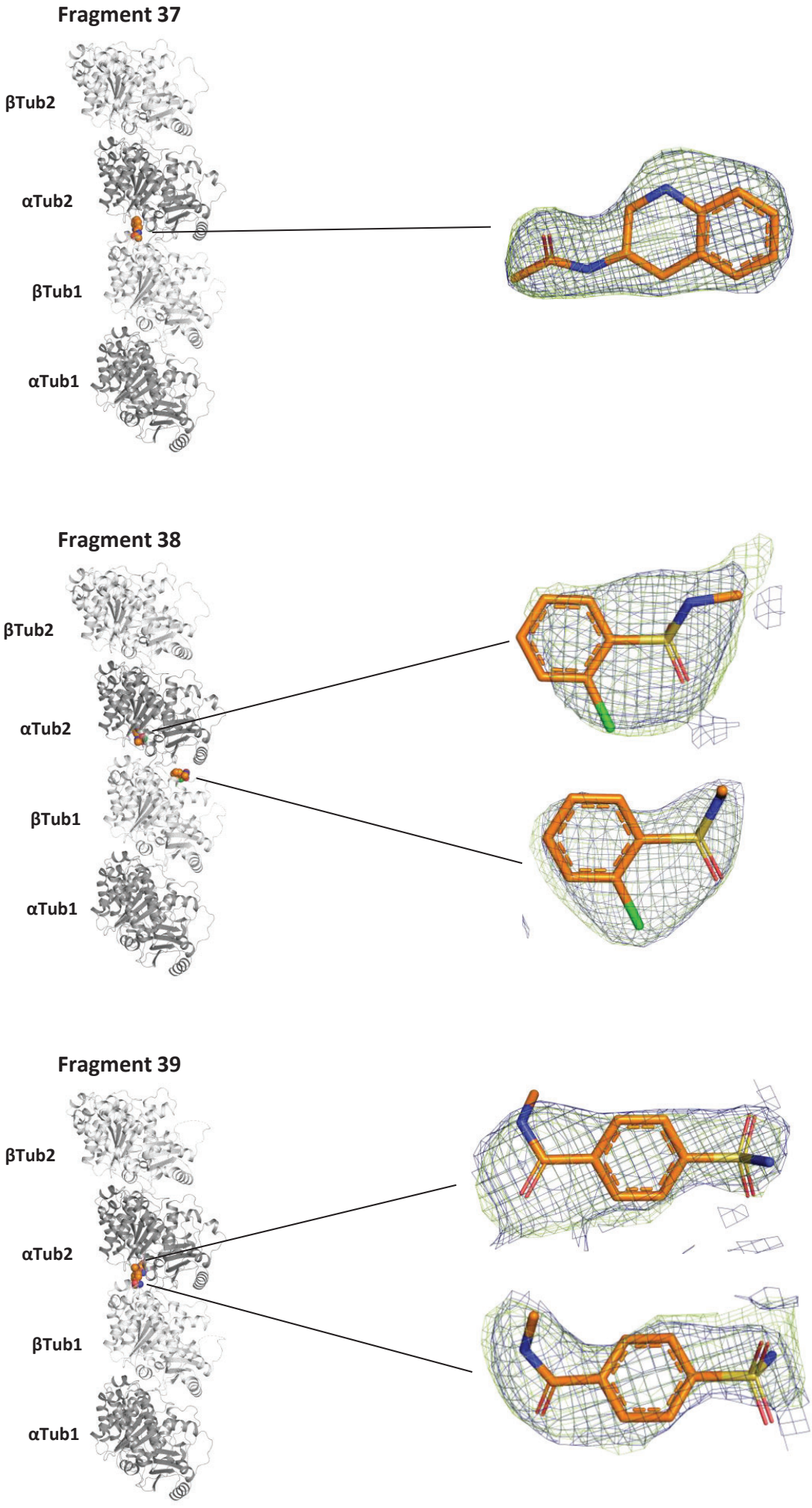

Figure S2 (continued)

Fragment 40

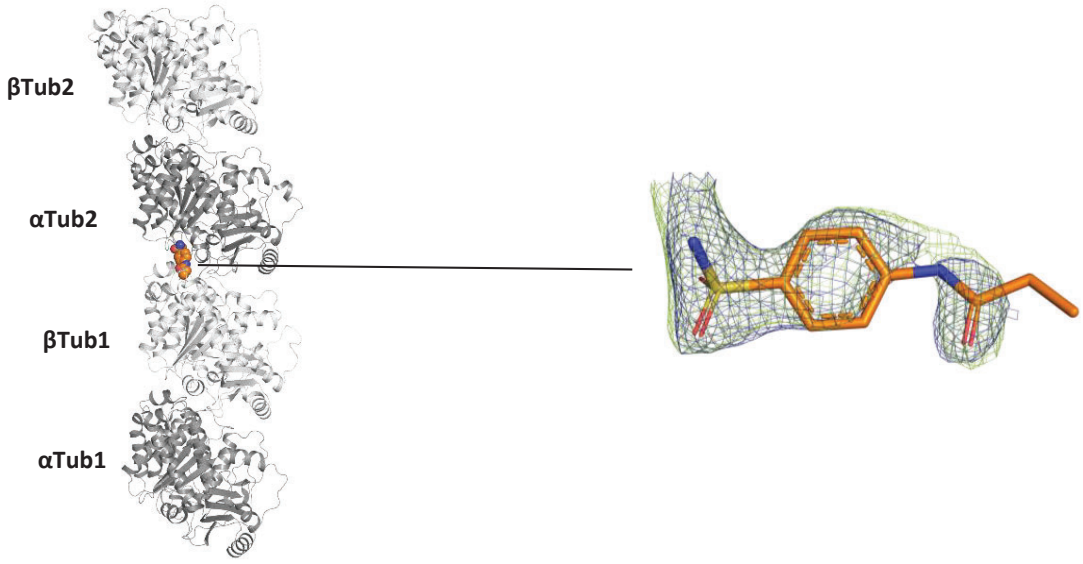

Fragment 41

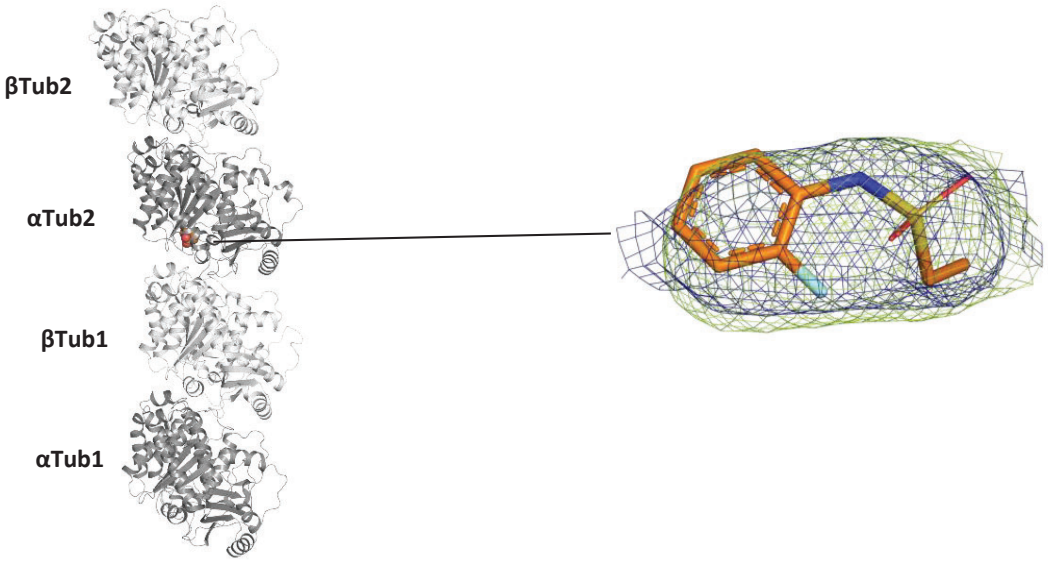

Fragment 42

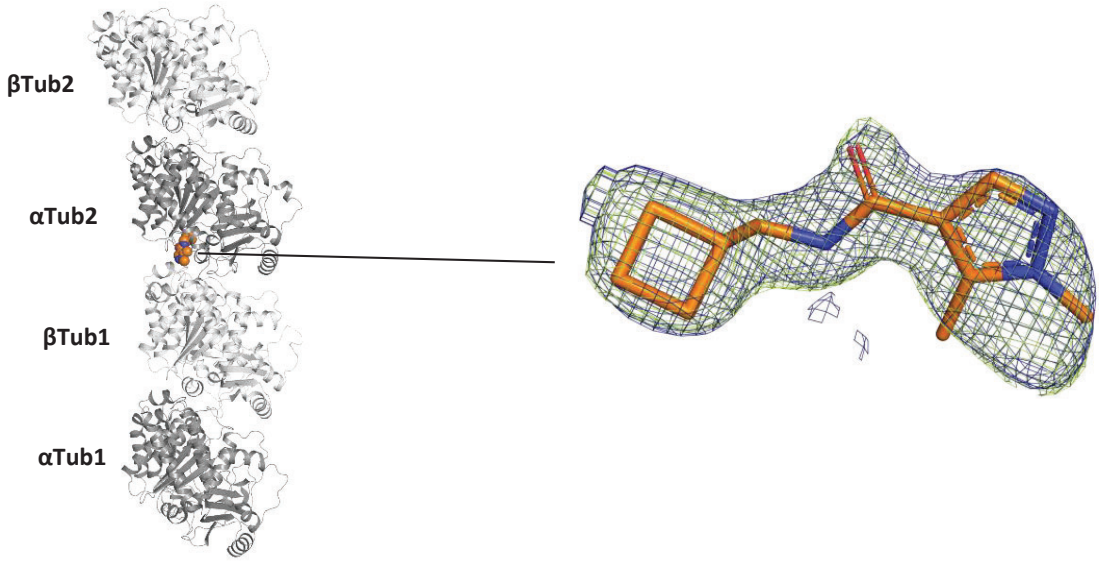

Figure S2 (continued)

Fragment 43

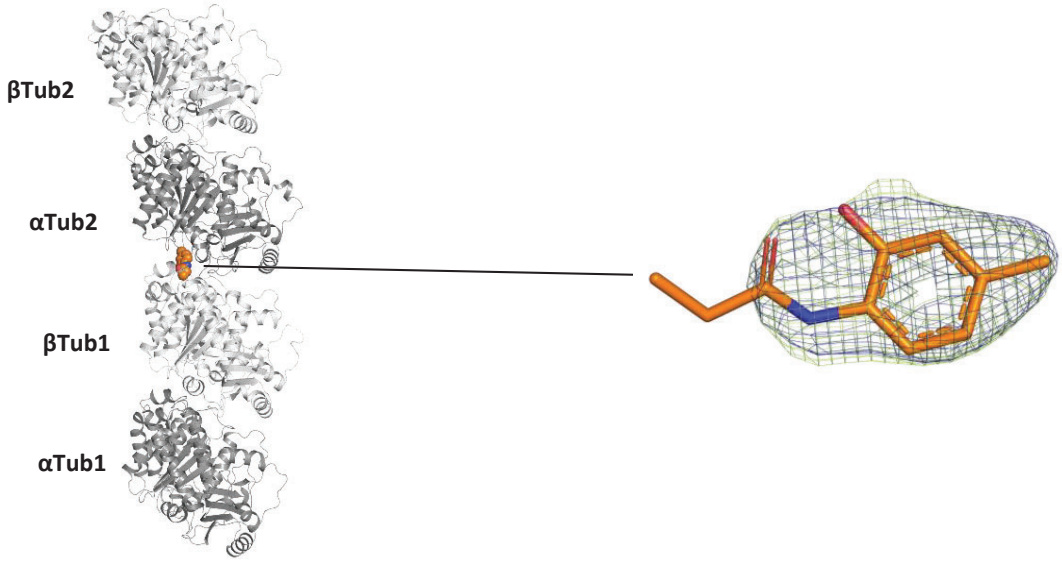

Fragment 44

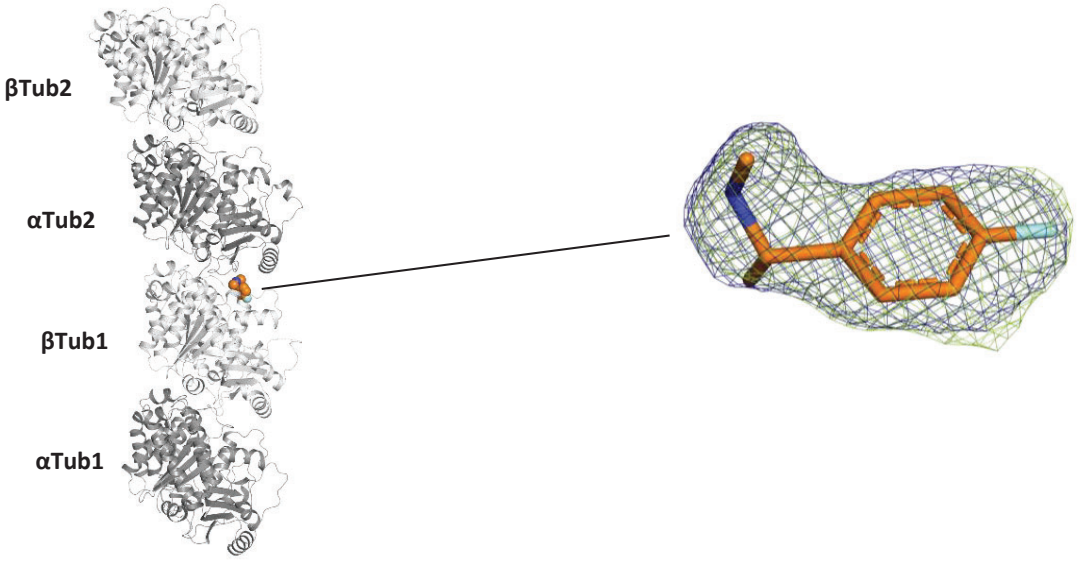

Fragment 45

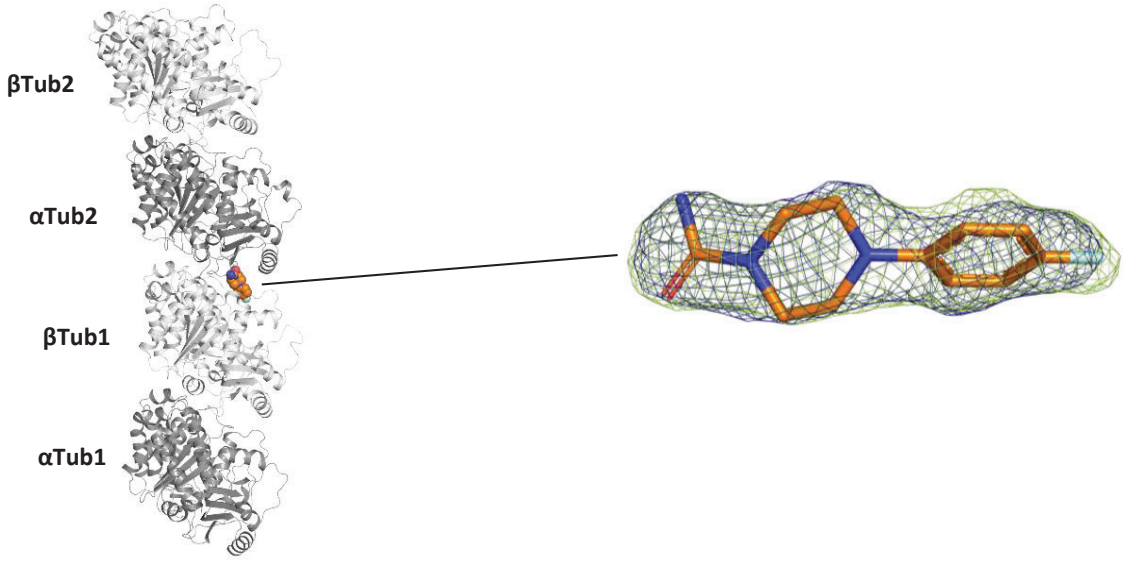

Figure S2 (continued)

Fragment 46

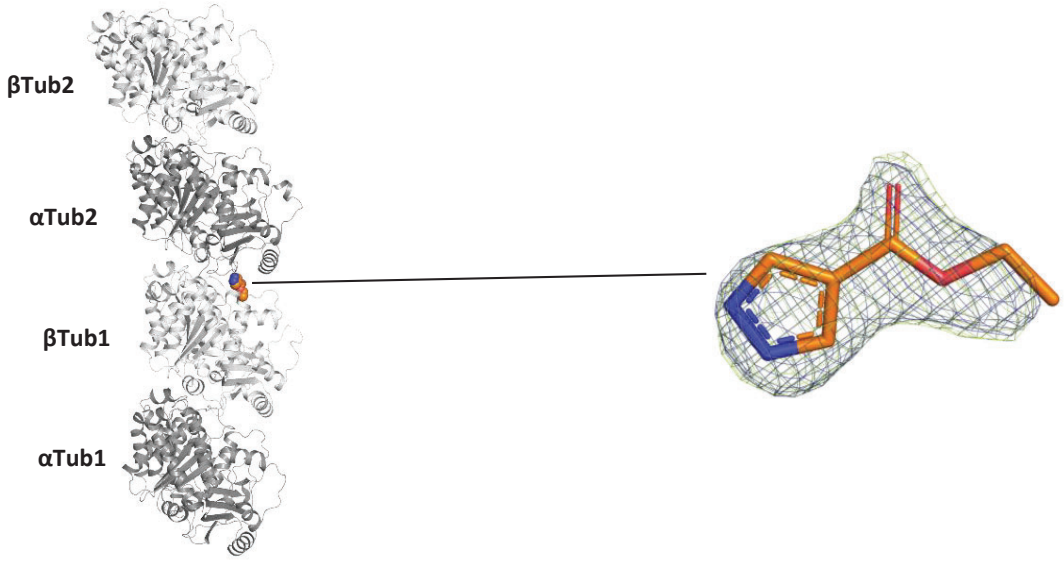

Fragment 47

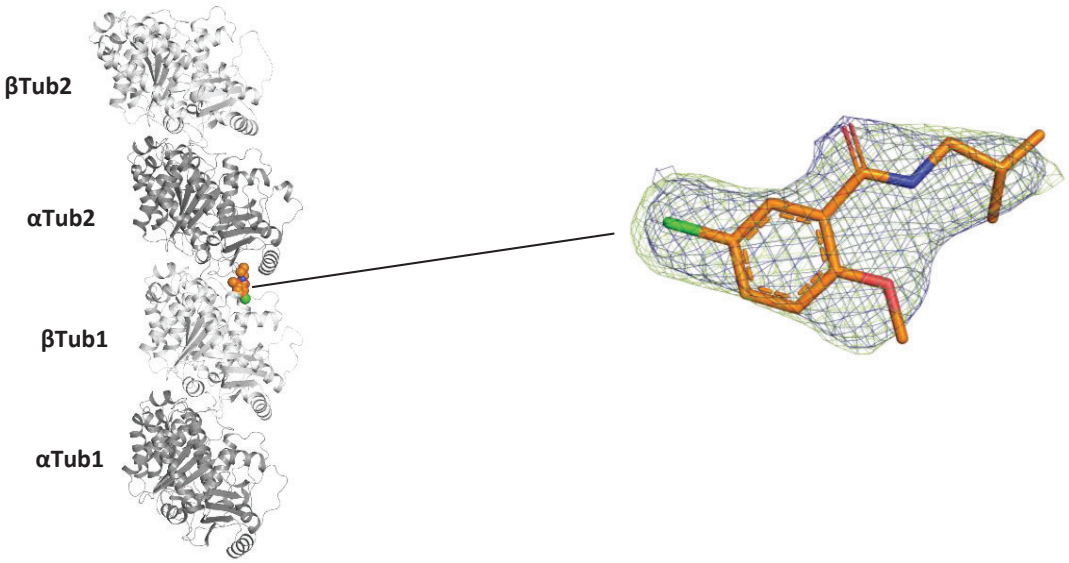

Fragment 48

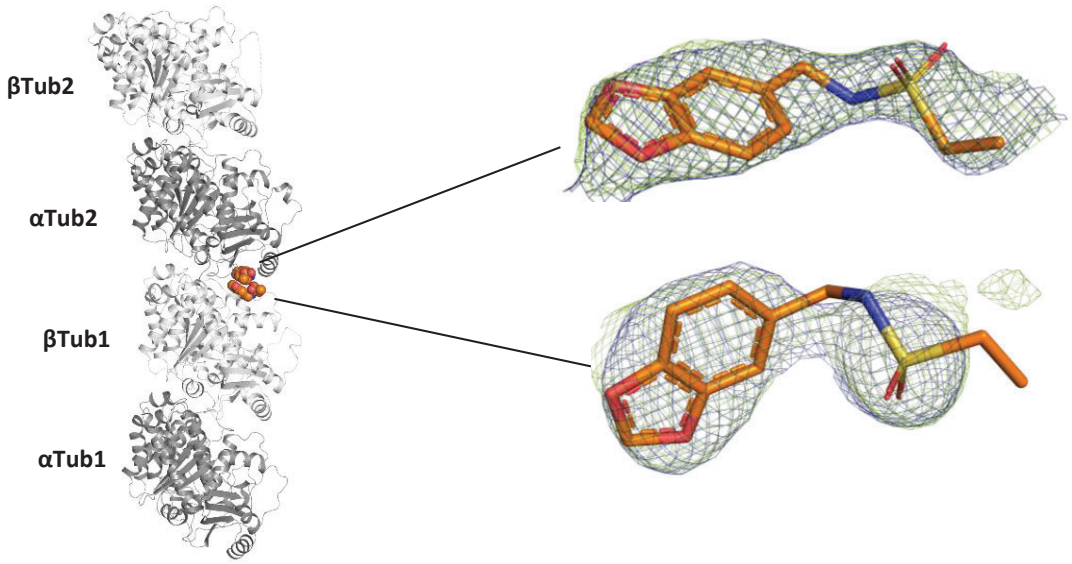

Figure S2 (continued)

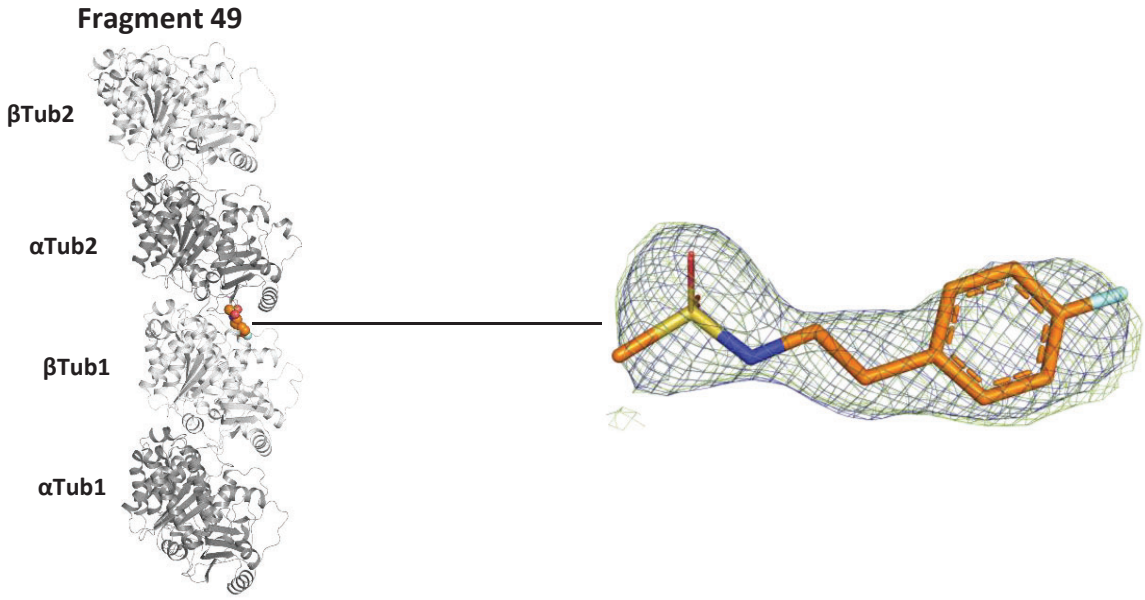

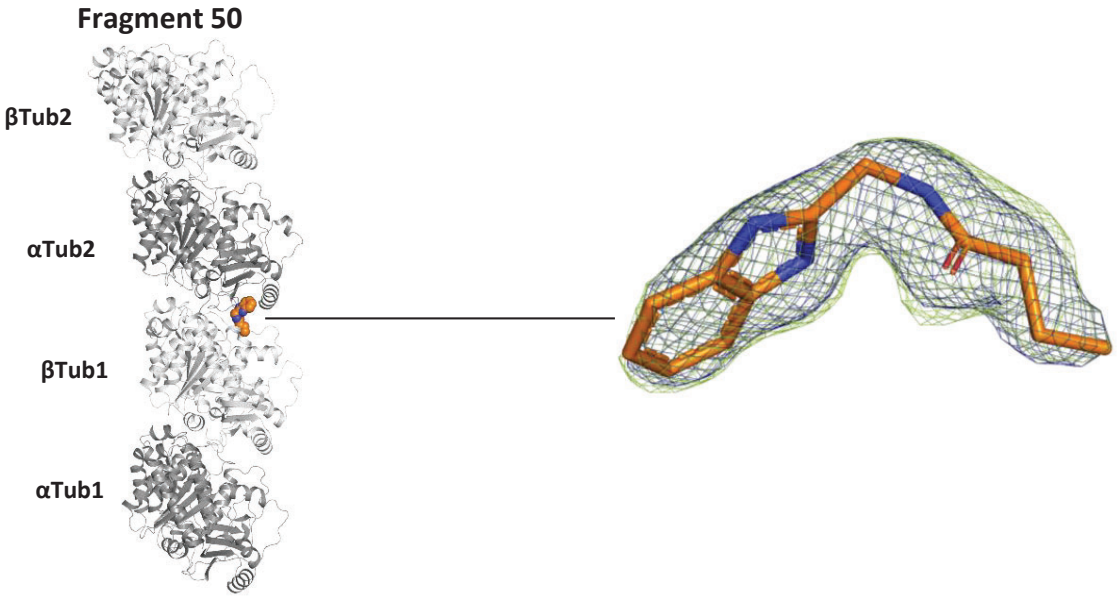

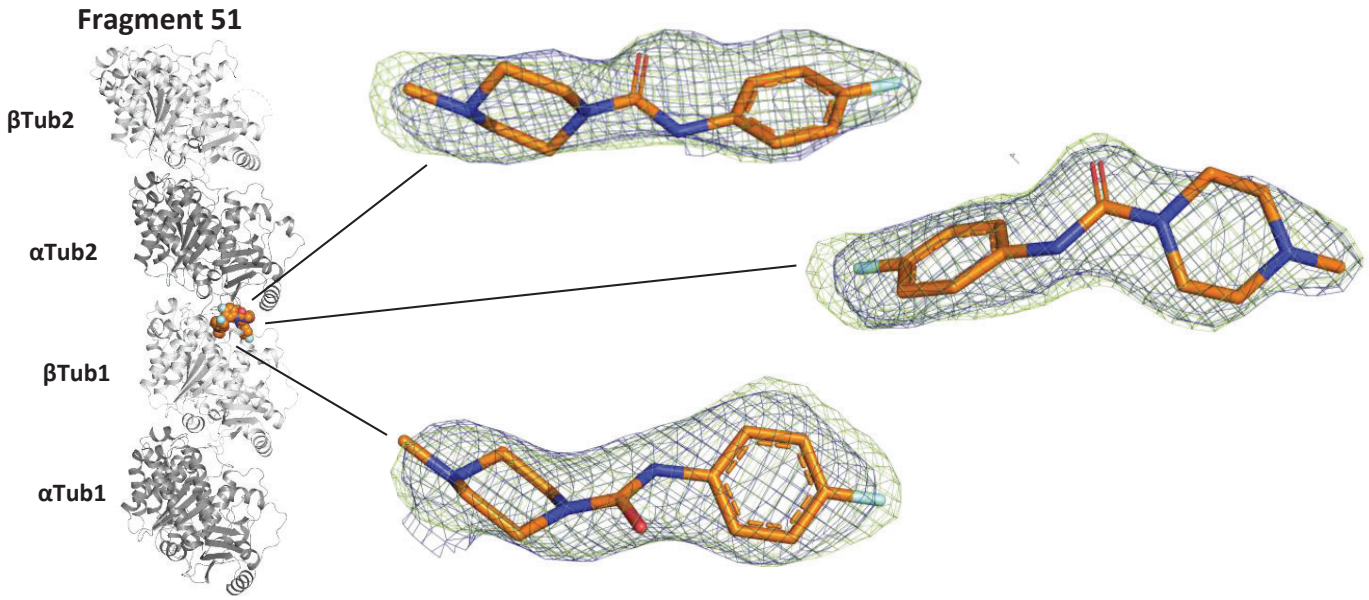

Figure S2 (continued)

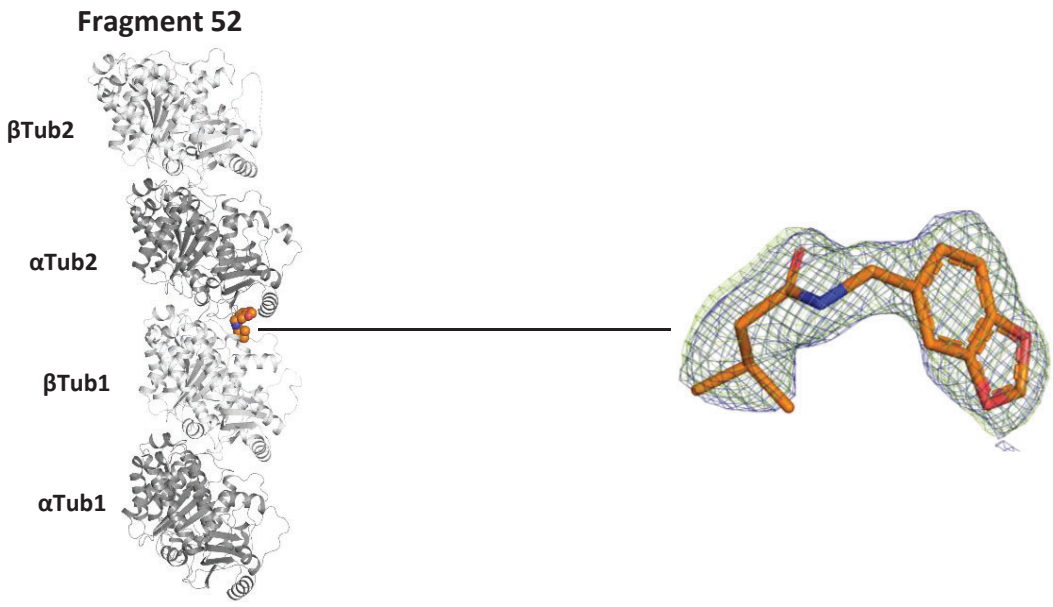

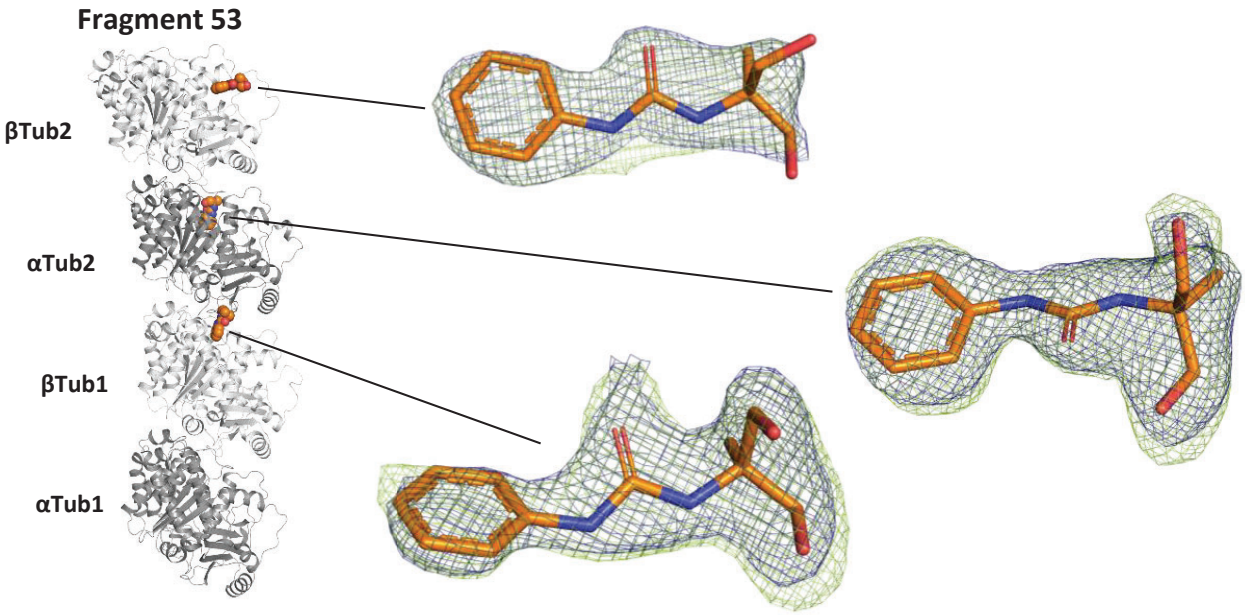

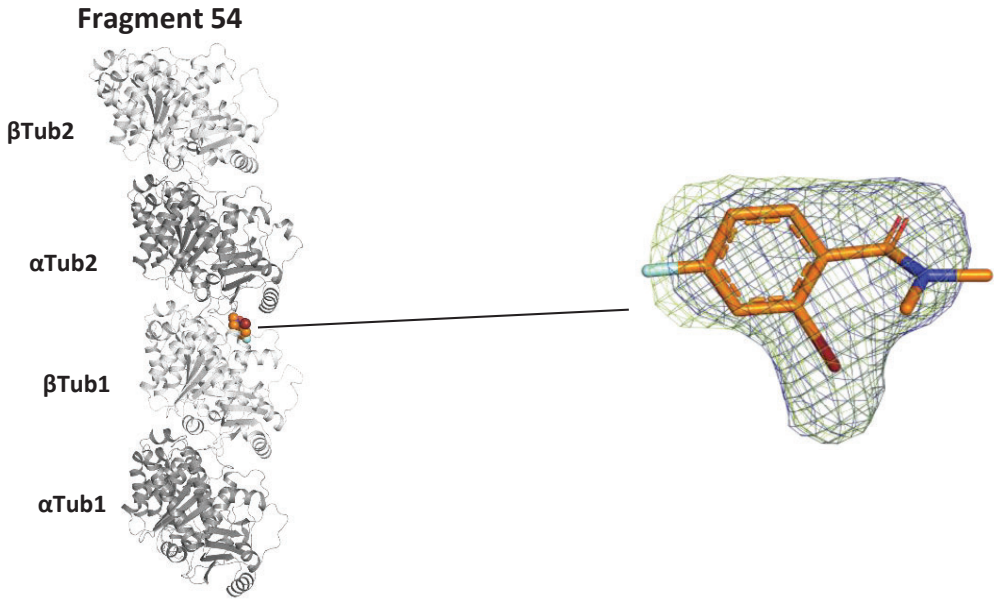

Figure S2 (continued)

Fragment 55

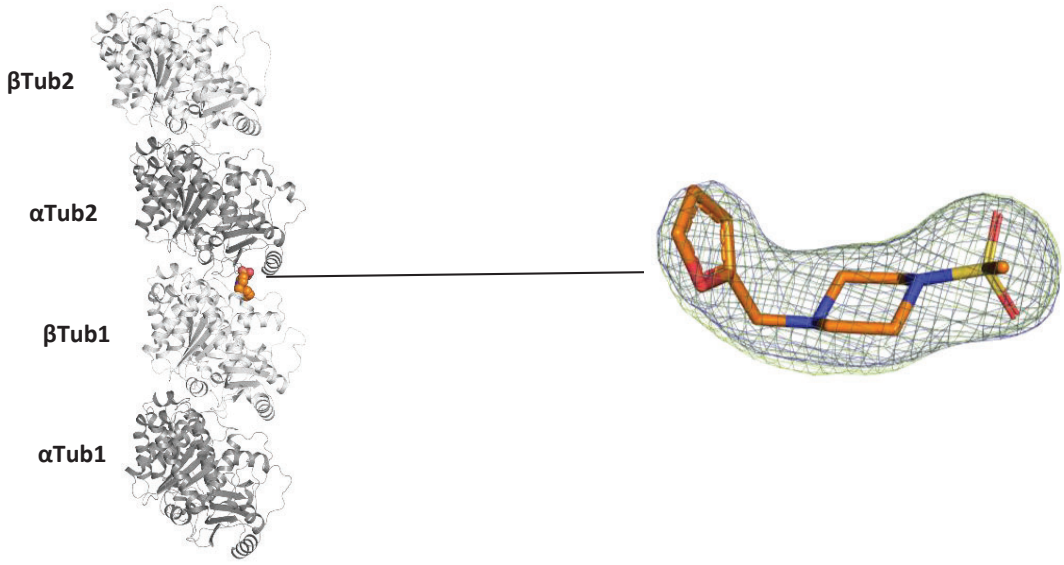

Fragment 56

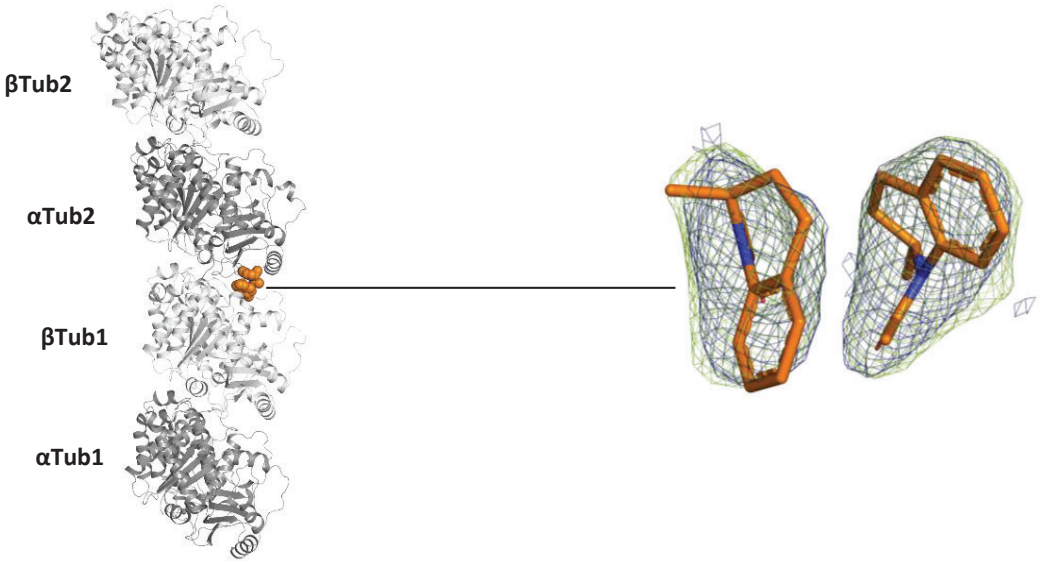

Fragment 57

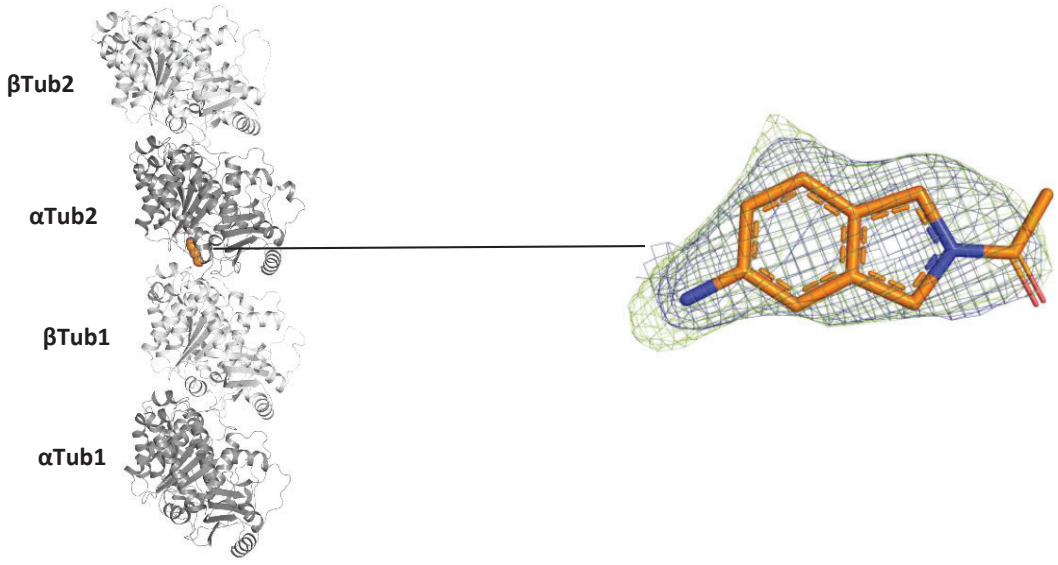

Figure S2 (continued)

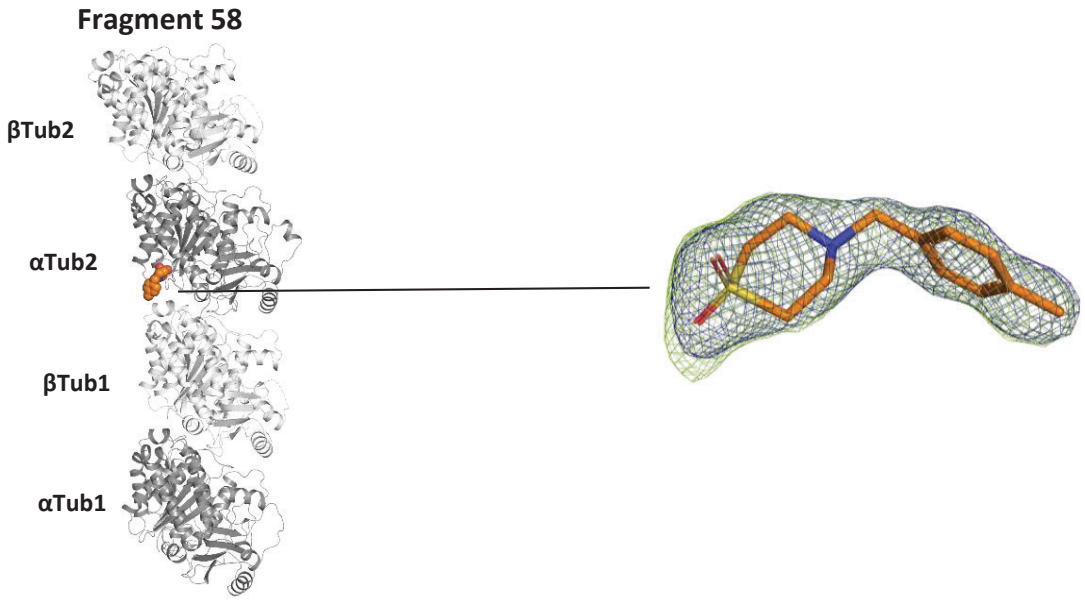

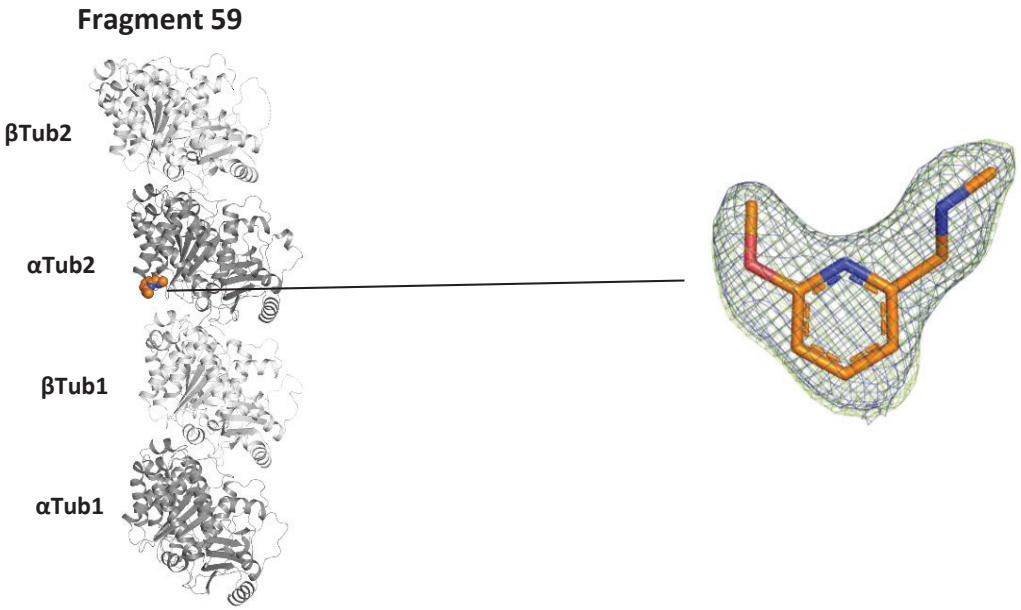

Figure S3

β-Tubulin

sID βI

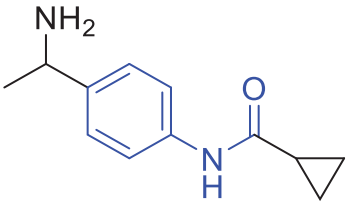

Fragment 01

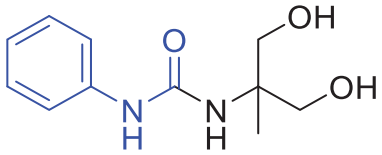

Fragment 53, also binds to sID βI and αII

sID βII

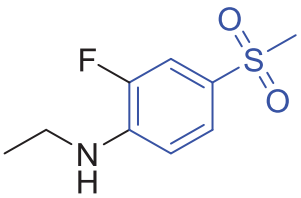

Fragment 02, also binds to sID αII

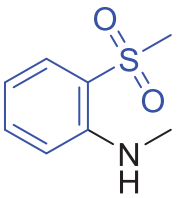

Fragment 03, also binds to sID βIV and βαIII

sID βIII

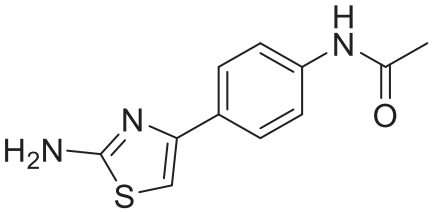

Fragment 04, also binds to sID βαII

sID βIV

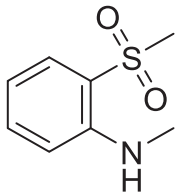

Fragment 03, also binds to sID βII and βαIII

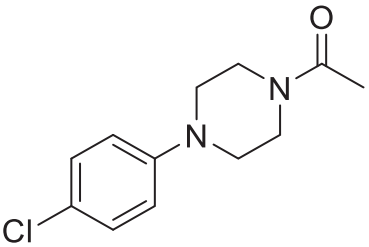

Fragment 05, also binds to sID αI, βαIII and X2

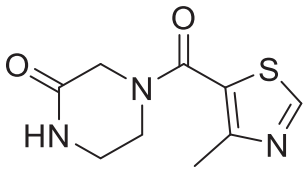

Fragment 06

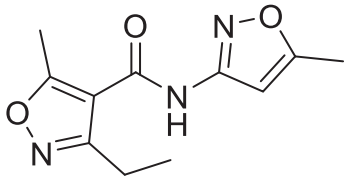

Fragment 07 (binds twice), also binds to sID βαIII

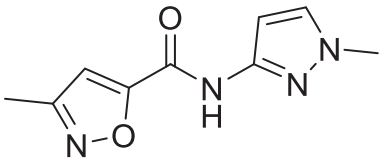

Fragment 08 (binds twice)

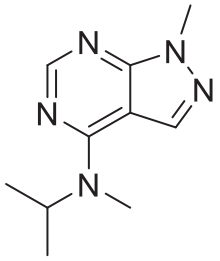

Fragment 09

Figure S3 (continued)

sID βIV continued

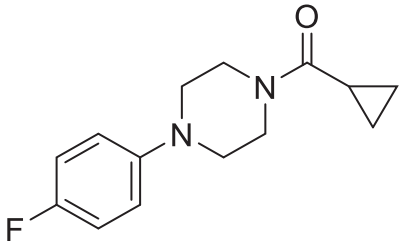

Fragment 10

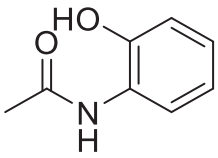

Fragment 11, also binds to sID βαII

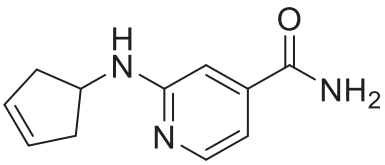

Fragment 12

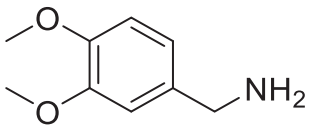

Fragment 13 (binds twice)

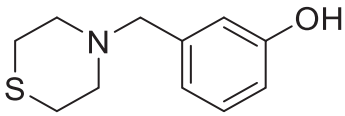

Fragment 14, also binds to sID βV

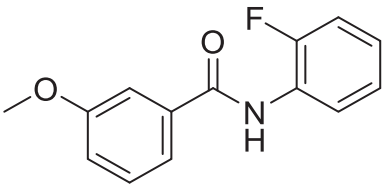

Fragment 15, also binds to sID βαIII

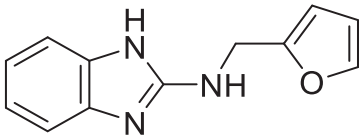

Fragment 16

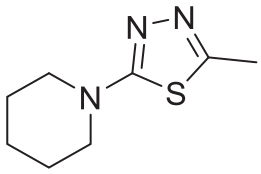

Fragment 17 (binds twice)

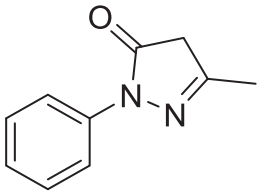

Fragment 18 (binds twice)

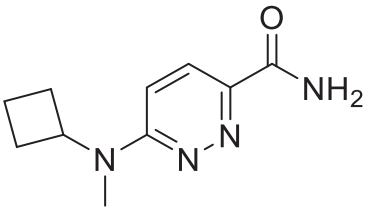

Fragment 19

sID βV

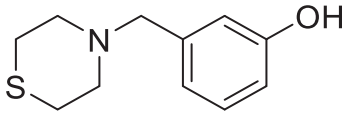

Fragment 14, also binds to sID βIV

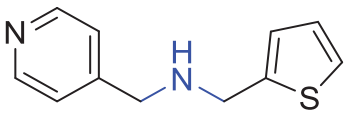

Fragment 20

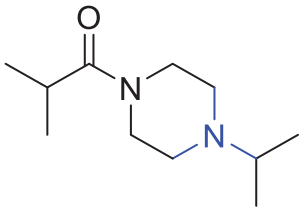

Fragment 21

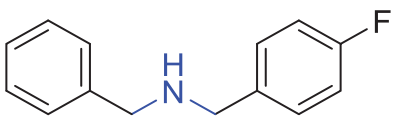

Fragment 22, also binds to sID βαIII

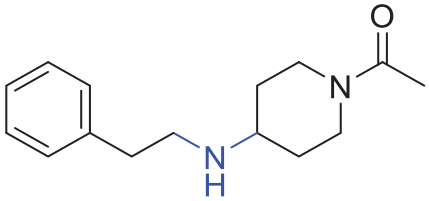

Fragment 23

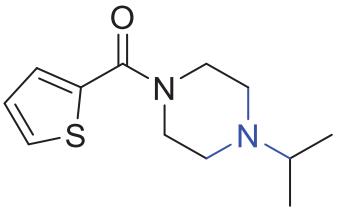

Fragment 24

Figure S3 (continued)

sID βV continued

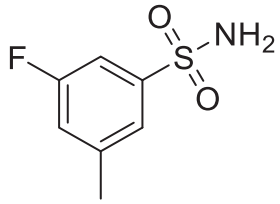

Fragment 25, also binds to sID αII

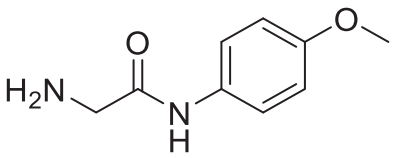

Fragment 26 (binds twice), also binds to sID βαIII and X1

β1α2-Tubulin

sID βαI

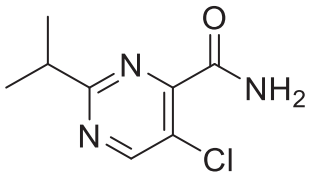

Fragment 27

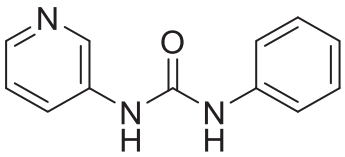

Fragment 28 (binds twice)

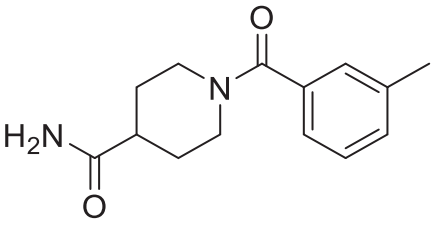

Fragment 29, also binds to sID βαIII

sID βαII

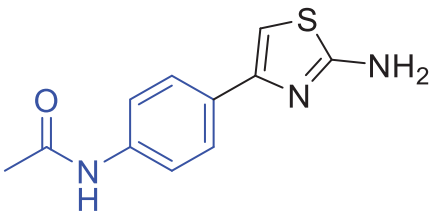

Fragment 04, also binds to sID βIII

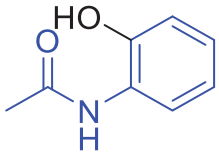

Fragment 11, also binds to sID βIV

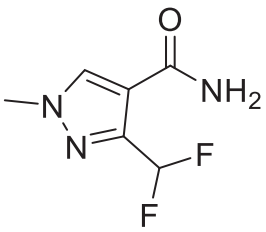

Fragment 30, also binds to sID βαIII

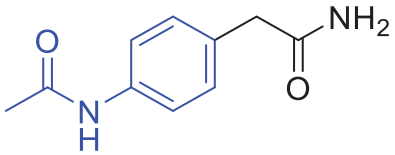

Fragment 31

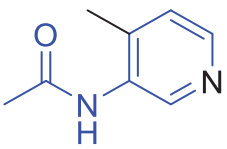

Fragment 32

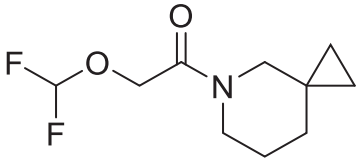

Fragment 33

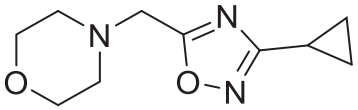

Fragment 34

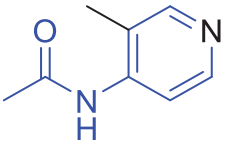

Fragment 35

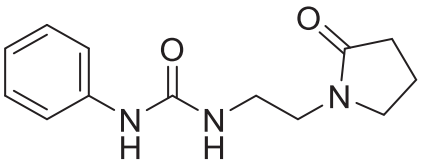

Fragment 36

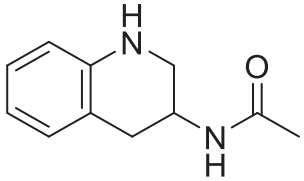

Fragment 37

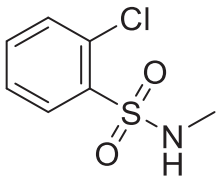

Fragment 38, also binds to sID βαIII

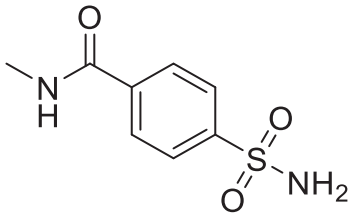

Fragment 39, also binds to sID X1

Figure S3 (continued)

sID βαII continued

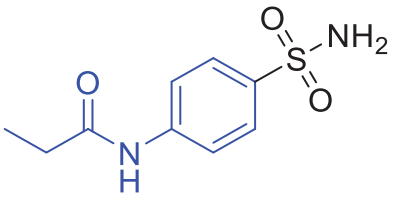

Fragment 40

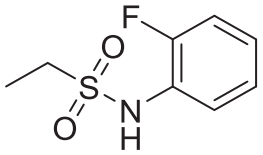

Fragment 41

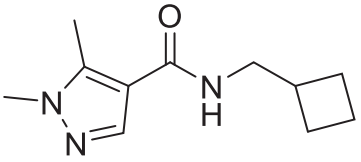

Fragment 42

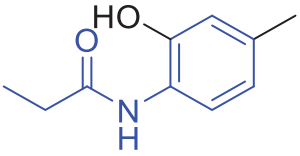

Fragment 43

sID βαIII

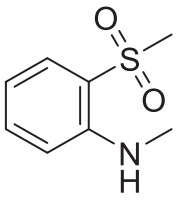

Fragment 03, also binds to sID βII and βIV

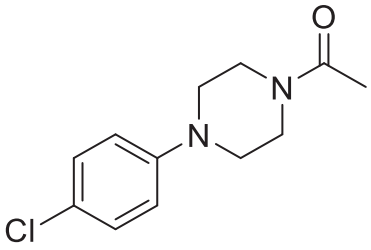

Fragment 05 (binds twice), also binds to sID αI, βIV and X2

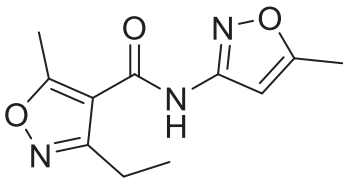

Fragment 07, also binds to sID βIV

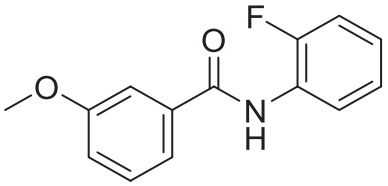

Fragment 15, also binds to sID βIV

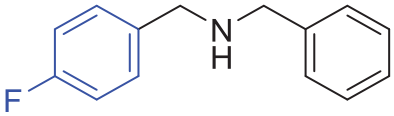

Fragment 22, also binds to sID βV

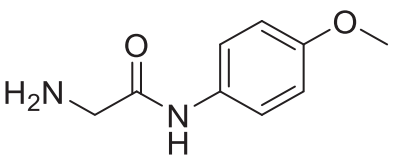

Fragment 26, also binds to sID βV and X1

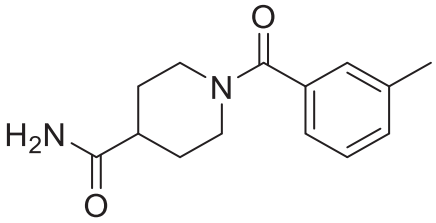

Fragment 29, also binds to sID βαI

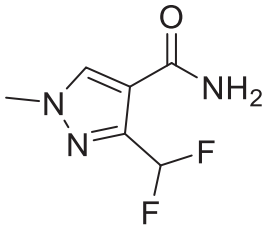

Fragment 30, also binds to sID βαII

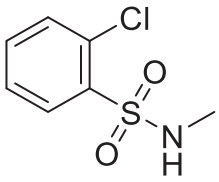

Fragment 38, also binds to sID βαII

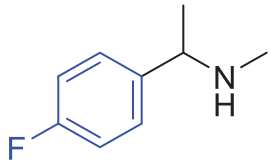

Fragment 44

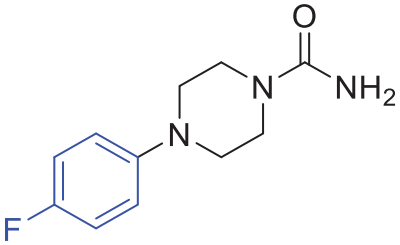

Fragment 45

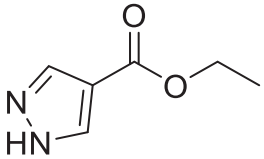

Fragment 46

Figure S3 (continued)

sID βαIII continued

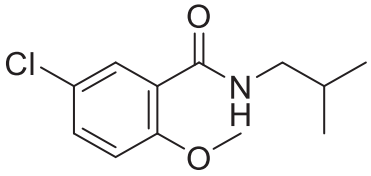

Fragment 47

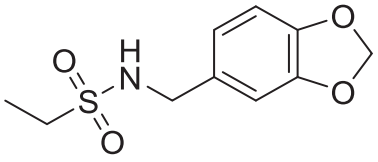

Fragment 48 (binds twice)

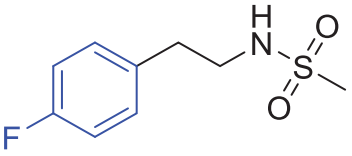

Fragment 49

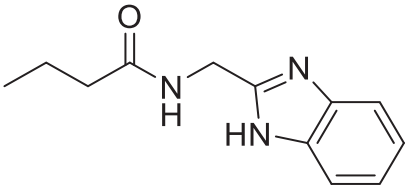

Fragment 50

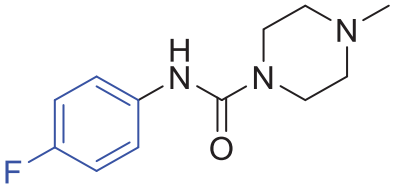

Fragment 51

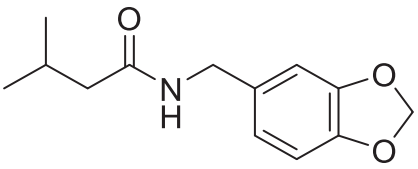

Fragment 52

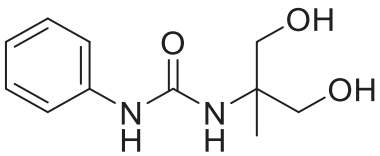

Fragment 53, also binds to sID βI and αII

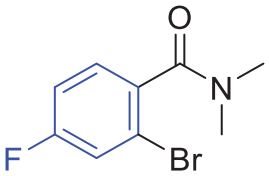

Fragment 54

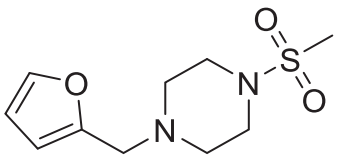

Fragment 55

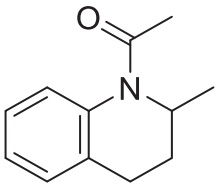

Fragment 56 (binds twice)

<u>α-Tubulin</u>

sID αI

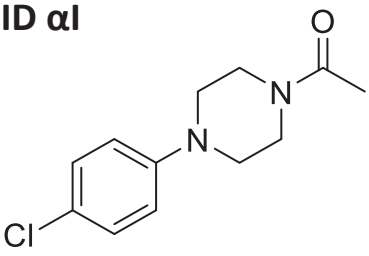

Fragment 05, also binds to sID βIV, βαIII and X2

sID αII

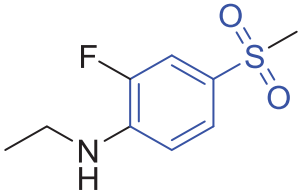

Fragment 02, also binds to sID βII

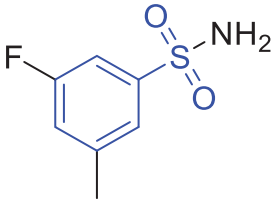

Fragment 25, also binds to sID βV

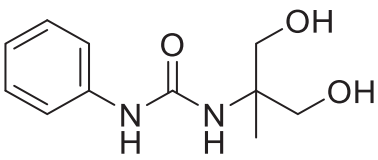

Fragment 53, also binds to sID βI and βαIII

Figure S3 (continued)

Crystal contact/binding partner in T_2R-TTL

sID X1

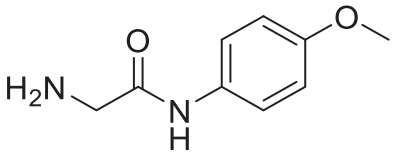

Fragment 26, also binds to sID βV and βαIII

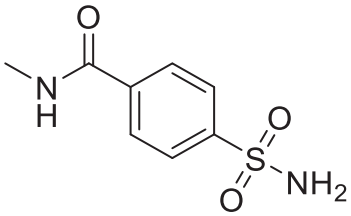

Fragment 39, also binds to sID βαII

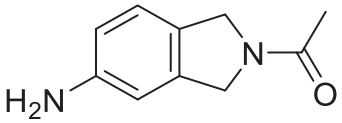

Fragment 57

sID X2

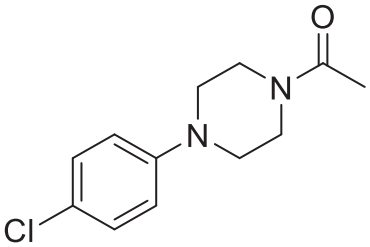

Fragment 05, also binds to sID αI, βIV and βαIII

sID X3

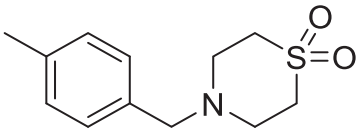

Fragment 58

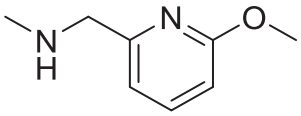

Fragment 59